

Review

On the numerical simulation of Bingham visco-plastic flow: Old and new results

Edward J. Dean^a, Roland Glowinski^{a,b}, Giovanna Guidoboni^{a,*}

^a Department of Mathematics, University of Houston, Houston, TX 77204-3476, United States

^b Laboratoire Jacques-Louis Lions, Université P. et M. Curie, 4 Place Jussieu, 75005 Paris, France

Received 5 April 2006; received in revised form 1 September 2006; accepted 1 September 2006

Abstract

The main goal of this article is to review various results and methods concerning the numerical simulation of Bingham visco-plastic flow; these results have been obtained from the early 1970s to now. We consider first the case of flow in cylindrical pipes and then flow in multi-dimensional cavities. The methods to be discussed include classical ones relying on regularization, (kind of) Lagrange multipliers and augmented Lagrangian techniques; they include also a duality–penalty method whose implementation relies on a Newton-Conjugate Gradient-Uzawa algorithm which seems to be new (in this context at least). Other issues are addressed; they concern particularly the accelerated calculation of steady state solutions and the time discretization of the unsteady flow models. The results of numerical experiments are presented, including the simulation of the wall driven flow in square cavities.

© 2006 Elsevier B.V. All rights reserved.

Keywords: Bingham flow; Numerical simulation; Operator splitting

Contents

1. Introduction	37
2. On the modeling of Bingham viscous plastic flow	37
3. Bingham flow in cylinders. (I) Formulation	38
4. Bingham flow in cylinders. (II) The regularization approach	39
5. Bingham flow in cylinders. (III) Variational inequality formulation. The multiplier approach	39
6. Bingham flow in cylinders. (IV) Time-discretization of problem (17)	40
7. Bingham flow in cylinders. (V) Steady flow	43
7.1. Formulation of the problem. Synopsis	43
7.2. Computing u_∞ via the solution of the time dependent problem	43
7.3. An iterative method à la Uzawa for the solution of problems (52) and (54)	44
7.4. A (pseudo-) time relaxation approach for the solution of problem (58), (59)	46
7.5. A penalty-Newton-Uzawa-conjugate gradient method for the solution of problem (58), (59)	48
8. Bingham flow in cylinders. (VI) An augmented Lagrangian approach to the solution of problem (58)	50
9. Bingham flow in cylinders. (VII) Finite element approximation	52
10. Bingham flow in cylinders. (VIII) Numerical experiments	52
11. Bingham flow in cavities	56
11.1. Generalities	56
11.2. Time-discretization of problem (6)–(9) by operator splitting	56
11.3. On the computer implementation of scheme (158)–(162)	57
11.4. Numerical experiments and further comments	58

* Corresponding author.

E-mail address: gio@math.uh.edu (G. Guidoboni).

12. Conclusions	61
Acknowledgment	61
References	61

1. Introduction

The numerical simulation of Bingham fluid flow has been the subject of intensive scrutiny for many years. We see at least two reasons for that:

- (i) The fact that materials as diverse as fresh concrete, tortilla dough, fruits-syrup mixtures, blood in the capillaries, muds used in drilling technologies, tooth pastes, . . . , have a Bingham medium behavior, namely: below a certain stress yield, the medium enjoys rigidity; above this yield the medium behaves like an incompressible viscous fluid.
- (ii) For applied mathematicians and numerical analysts, Bingham flow modeling has been a permanent source of challenging problems for many decades already, the main breakthrough in this direction being the variational inequality formulation due to Duvaut and Lions (Refs. [1,2]).

Our goal in this article is to review several of the approaches we are aware of, concerning the numerical simulation of Bingham flow. Roughly speaking, there exist two main approaches: one based on regularization procedures, the other based on the use of multipliers. There is no way that we can describe all the related methods in this article; we will discuss, nevertheless, quite a few of them, considering first the case of Bingham flow in cylindrical pipes and then the more general case of Bingham flow in multi-dimensional cavities.

It has become practically impossible to give all the references related to the modeling and simulation of Bingham fluid flow (more than 11,000 hits on Google Scholar); in addition to [1,2], let us mention, among many others, [3–6] (see also the references therein).

2. On the modeling of Bingham viscous plastic flow

The material in this section is pretty classical. It has been introduced here to fix the notation and to remind of some basic facts concerning the mathematical modeling of Bingham flow. Let thus Ω be a domain (i.e., an open and connected region) of \mathbb{R}^d ($d = 2$ or 3 in applications); we denote by Γ the boundary of Ω . The isothermal flow of an incompressible Bingham visco-plastic medium, during the time interval $(0, T)$, is modeled by the following system of equations (clearly of the Navier–Stokes type):

$$\varrho[\partial_t \mathbf{u} + (\mathbf{u} \cdot \nabla) \mathbf{u}] = \nabla \cdot \boldsymbol{\sigma} + \mathbf{f} \quad \text{in } \Omega \times (0, T), \tag{1}$$

$$\nabla \cdot \mathbf{u} = 0 \quad \text{in } \Omega \times (0, T), \tag{2}$$

$$\boldsymbol{\sigma} = -p\mathbf{I} + \sqrt{2}g \frac{\mathbf{D}(\mathbf{u})}{|\mathbf{D}(\mathbf{u})|} + 2\mu\mathbf{D}(\mathbf{u}), \tag{3}$$

$$\mathbf{u}(0) = \mathbf{u}_0 \quad (\text{with } \nabla \cdot \mathbf{u}_0 = 0). \tag{4}$$

For simplicity, we shall consider only Dirichlet boundary conditions, namely:

$$\mathbf{u} = \mathbf{u}_B \quad \text{on } \Gamma \times (0, T), \quad \text{with } \int_{\Gamma} \mathbf{u}_B(t) \cdot \mathbf{n} \, d\Gamma = 0, \text{ a.e. on } (0, T). \tag{5}$$

In systems (1)–(5):

- ϱ (resp., μ and g) is the density (resp., are the viscosity and plasticity yield) of the Bingham medium; we have $\varrho > 0$, $\mu > 0$ and $g > 0$.
- \mathbf{f} is a density of external forces.
- $\mathbf{D}(\mathbf{v}) = \frac{1}{2}[\nabla \mathbf{v} + (\nabla \mathbf{v})^t] (= D_{ij}(\mathbf{v})_{1 \leq i, j \leq d})$, $\forall \mathbf{v} \in (H^1(\Omega))^d$, and $|\mathbf{D}(\mathbf{v})|$ is the Frobenius norm of tensor $\mathbf{D}(\mathbf{v})$, i.e.,

$$|\mathbf{D}(\mathbf{v})| = \left(\sum_{1 \leq i, j \leq d} |D_{ij}(\mathbf{v})|^2 \right)^{1/2}.$$

- \mathbf{n} is the outward unit normal vector at Γ .
- We have denoted (and will denote later on) by $\varphi(t)$ the function $x \rightarrow \varphi(x, t)$.

We observe that if $g = 0$, systems (1)–(5) reduces to the Navier–Stokes equations modeling isothermal incompressible Newtonian viscous fluid flow. Having said that, if $g > 0$ the above model makes no sense on the (rigid) set

$$Q_0 = \{\{x, t\} | \{x, t\} \in \Omega \times (0, T), \mathbf{D}(\mathbf{u})(x, t) = \mathbf{0}\}.$$

Following Duvaut and Lions (Refs. ([1], Chapter 6) and ([2], Chapter 6)) we eliminate the above difficulty by considering instead of the (doubly) nonlinear systems (1)–(5) the following *variational inequality model* (where $dx = dx_1 \dots dx_d$):

Find $\{\mathbf{u}(t), p(t)\} \in (H^1(\Omega))^d \times L^2(\Omega)$ such that a.e. on $(0, T)$ we have

$$\begin{aligned} \varrho \int_{\Omega} \partial_t \mathbf{u}(t) \cdot (\mathbf{v} - \mathbf{u}(t)) dx + \varrho \int_{\Omega} (\mathbf{u}(t) \cdot \nabla) \mathbf{u}(t) \cdot (\mathbf{v} - \mathbf{u}(t)) dx + \mu \int_{\Omega} \nabla \mathbf{u}(t) : \nabla (\mathbf{v} - \mathbf{u}(t)) dx + \sqrt{2}g(j(\mathbf{v}) - j(\mathbf{u}(t))) \\ - \int_{\Omega} p(t) \nabla \cdot (\mathbf{v} - \mathbf{u}(t)) dx \geq \int_{\Omega} \mathbf{f}(t) \cdot (\mathbf{v} - \mathbf{u}(t)) dx, \quad \forall \mathbf{v} \in \mathbf{V}_B(t) \end{aligned} \quad (6)$$

$$\nabla \cdot \mathbf{u}(t) = 0 \quad \text{in } \Omega, \quad (7)$$

$$\mathbf{u}(0) = \mathbf{u}_0, \quad (8)$$

$$\mathbf{u}(t) = \mathbf{u}_B(t) \quad \text{on } \Gamma, \quad (9)$$

with, in (6),

$$j(\mathbf{v}) = \int_{\Omega} |\mathbf{D}(\mathbf{v})| dx, \quad \forall \mathbf{v} \in (H^1(\Omega))^d \quad (10)$$

and

$$\mathbf{V}_B(t) = \{\mathbf{v} | \mathbf{v} \in (H^1(\Omega))^d, \mathbf{v} = \mathbf{u}_B(t) \text{ on } \Gamma\}. \quad (11)$$

Various comments concerning formulation (6)–(9) can be found in, e.g., Ref. ([7], Chapter 10). The variational inequality formulation of temperature dependent Bingham flow can be found in, e.g., Ref. [8].

In the following sections we are going to review a variety of computational techniques which have been developed during the last four decades for the solution of problems (1)–(5) and (6)–(9). For simplicity, we will start our discussion with Bingham flow in cylinders, and then consider flow in bounded multidimensional cavities.

Remark 1. It follows from Refs. [1] and [2] that there exists a tensor-valued function λ such that the formulation (6)–(9) is equivalent to

$$\varrho[\partial_t \mathbf{u} + (\mathbf{u} \cdot \nabla) \mathbf{u}] = \nabla \cdot \boldsymbol{\sigma} \quad \text{in } \Omega \times (0, T), \quad \nabla \cdot \mathbf{u} = 0 \quad \text{in } \Omega \times (0, T), \quad \mathbf{u} = \mathbf{u}_B \text{ on } \Gamma \times (0, T), \quad \mathbf{u}(0) = \mathbf{u}_0 \quad (12)$$

with

$$\boldsymbol{\sigma} = 2\mu \mathbf{D}(\mathbf{u}) + g\sqrt{2} \boldsymbol{\lambda}, \quad (13)$$

$$\boldsymbol{\lambda} : \mathbf{D}(\mathbf{u}) = |\mathbf{D}(\mathbf{u})|, \quad \boldsymbol{\lambda} = \boldsymbol{\lambda}^t, \quad |\boldsymbol{\lambda}| \leq 1. \quad (14)$$

We can take advantage of the above formulation to solve (6)–(9) numerically as shown in Section 7.2. Incidentally, assuming that λ is known, relation (13) provides the stress tensor everywhere in $\Omega \times (0, T)$ (this includes the rigid region Q_0). The tensor-valued function $g\sqrt{2}\lambda$ can be viewed as the extra-stress tensor associated to the visco-plastic behavior of the medium.

3. Bingham flow in cylinders. (I) Formulation

The isothermal and unsteady axial flow of an incompressible visco-plastic Bingham fluid in an infinitely long cylinder of (bounded) cross-section Ω is (formally) modeled by the following nonlinear parabolic equation (where Γ is the boundary of Ω):

$$\varrho \partial_t u - \mu \nabla^2 u - g \nabla \cdot \left(\frac{\nabla u}{|\nabla u|} \right) = C \quad \text{in } \Omega \times (0, T), \quad u = 0 \text{ on } \Gamma \times (0, T), \quad u(0) = u_0. \quad (15)$$

In system (15): (i) u is the axial flow velocity, i.e., $\mathbf{u} = \{0, 0, u\}$, assuming that the fluid flows in the Ox_3 -direction, Ω being parallel to the (Ox_1, Ox_2) -plane. (ii) C is the pressure drop per unit length (it is a function of t , only, and possibly a constant). System (15) is a particular case of (1)–(5).

Before going further, let us observe that (as in Section 2, for (1)–(5)), model (15) makes no sense in the (space-time) rigid region

$$Q_0 = \{\{x, t\} | \{x, t\} \in \Omega \times (0, T), \nabla u(x, t) = \mathbf{0}\}.$$

There are classically two approaches to overcome the above difficulty, namely the regularization and multiplier approaches.

4. Bingham flow in cylinders. (II) The regularization approach

Let ε be a small positive parameter. The idea here is to replace (12) by the following well-posed nonlinear parabolic problem:

$$\varrho \partial_t u_\varepsilon - \mu \nabla^2 u_\varepsilon - g \nabla \cdot \left(\frac{\nabla u_\varepsilon}{(\varepsilon^2 + |\nabla u_\varepsilon|^2)^{1/2}} \right) = C \quad \text{in } \Omega \times (0, T), \quad u_\varepsilon = 0 \text{ on } \Gamma \times (0, T), \quad u_\varepsilon(0) = u_0. \quad (16)$$

We will return later on the approximation properties of u_ε . Let us say that the above regularization procedure has been widely used, not only in Visco-Elasticity, but also in Image Processing (see, e.g. Ref. [9] and the references therein). It has however some drawbacks, a major one being that if $C = 0$, the well-known property that $u(t) \rightarrow 0$ in finite time is lost. An alternative to regularization is provided by the *multiplier approach*, to be discussed in the following section.

Remark 2. Other regularization procedures can be found in Ref. [29].

5. Bingham flow in cylinders. (III) Variational inequality formulation. The multiplier approach

It follows from Refs. [1] and [2] that a mechanically and mathematically correct formulation of problem (15) is provided by the following variational inequality type model:

$$\begin{aligned} u(t) &\in H_0^1(\Omega) \text{ a.e. on } (0, T), & \varrho \int_\Omega \partial_t u(v - u) \, dx + \mu \int_\Omega \nabla u \cdot \nabla(v - u) \, dx + g(j(v) - j(u)) &\geq C \int_\Omega (v - u) \, dx, \\ \forall v &\in H_0^1(\Omega), & u(0) &= u_0, \end{aligned} \quad (17)$$

with

$$j(v) = \int_\Omega |\nabla v| \, dx. \quad (18)$$

The following mathematical results hold, all important from a computational point of view:

Theorem 1. Let u and u_ε be the respective solutions of problem (17) and (16); we have then, if $u_0 \in L^2(\Omega)$,

$$\|u_\varepsilon(t) - u(t)\|_{L^2(\Omega)} \leq \left(\frac{g|\Omega|}{\mu\lambda_0} \right)^{1/2} \left[1 - \exp\left(-\frac{2\mu\lambda_0}{\varrho}t\right) \right]^{1/2} \sqrt{\varepsilon}, \quad \forall t \in [0, T], \quad (19)$$

with $|\Omega| = \text{meas.}(\Omega)$, and $\lambda_0 > 0$ the smallest eigenvalue of the operator $-\nabla^2$ on Ω for the homogeneous Dirichlet boundary conditions.

We have thus

$$\lim_{\varepsilon \rightarrow 0} u_\varepsilon = u \text{ in } L^\infty(0, T; L^2(\Omega)). \quad (20)$$

The convergence properties (19) and (20) provide, quite clearly, a justification of the regularization procedure described in Section 4.

Theorem 2. Suppose that C is also constant in time and that $T = +\infty$. We have then, if $u_0 \in L^2(\Omega)$, the following asymptotic behavior:

$$u(t) = 0, \quad \forall t > T_c \text{ if } C < g\gamma|\Omega|^{-1/2}, \quad (21)$$

where

$$\gamma = \inf_v \left[\frac{\int_\Omega |\nabla v| \, dx}{\|v\|_{L^2(\Omega)}} \right], \quad v \in H_0^1(\Omega) \setminus \{0\},$$

and

$$T_c = \frac{\varrho}{\mu\lambda_0} \ln \left[1 + \frac{\mu\lambda_0 \|u_0\|_{L^2(\Omega)}}{\gamma g - C|\Omega|^{1/2}} \right]. \quad (22)$$

If $C \geq \gamma g|\Omega|^{-1/2}$, then the following estimate holds:

$$\|u(t) - u_\infty\|_{L^2(\Omega)} \leq \|u_0 - u_\infty\|_{L^2(\Omega)} \exp\left(-\frac{\mu\lambda_0 t}{\varrho}\right), \quad (23)$$

with u_∞ the corresponding steady-state solution.

The estimate provided by (23) is not optimal since it does not include g (the plasticity yield).

Theorem 3. *The solution of problem (17) is characterized by the existence of a vector-valued function $\lambda (= \{\lambda_1, \lambda_2\})$ such that*

$$\begin{aligned} \rho \partial_t u - \mu \nabla^2 u - g \nabla \cdot \lambda &= C \text{ in } \Omega \times (0, T), \quad u = 0 \text{ on } \Gamma \times (0, T), \quad |\lambda(x, t)| \leq 1, \text{ a.e. on } \Omega \times (0, T) \text{ and } \lambda \cdot \nabla u = |\nabla u|, \\ u(0) &= u_0, \end{aligned} \quad (24)$$

with $|\mathbf{q}| = (q_1^2 + q_2^2)^{1/2}$.

Theorem 3 is proved in, e.g., Refs. [1,2]. Actually, there are several ways to prove the above theorem: non-constructive ones relying on the Hahn–Banach Theorem, and more constructive ones based on the regularization procedure briefly discussed in Section 4 (the regularization approach has been used in Ref. ([10], Chapter 2) to prove the steady state analogue of **Theorem 3**). Further observations are in order; among them:

Remark 3. Without being (strictly speaking) a Lagrange (or Kuhn–Tucker) multiplier, the vector λ shares many properties with such vectors, explaining why we will call it a multiplier in the sequel. Among its properties, let us emphasize that the multiplier λ is non-unique (as shown in, e.g., Refs. [11,12]), however $\nabla \cdot \lambda$ is unique.

Remark 4. The third relations in (24) are equivalent to

$$\lambda(t) = P_{\Lambda}[\lambda(t) + rg \nabla u(t)], \quad \forall r \geq 0, \quad (25)$$

with the closed convex set Λ and the projection operator $P_{\Lambda} : (L^2(\Omega))^2 \rightarrow \Lambda$ defined by

$$\Lambda = \{\mathbf{q} | \mathbf{q} \in (L^2(\Omega))^2, |\mathbf{q}(x)| \leq 1, \text{ a.e. on } \Omega\} \quad (26)$$

and

$$P_{\Lambda}(\mathbf{q})(x) = \frac{\mathbf{q}(x)}{\max(1, |\mathbf{q}(x)|)}, \text{ a.e. on } \Omega, \quad \forall \mathbf{q} \in (L^2(\Omega))^2, \quad (27)$$

respectively. The present remark has important computational implications, as shown in Section 7.2.

6. Bingham flow in cylinders. (IV) Time-discretization of problem (17)

To the best of our knowledge, the backward Euler scheme, described below, is the only scheme preserving the asymptotic behavior of the solution of the continuous problem (namely, problem (17)), including the return to rest in finite time (if g is large enough). This scheme reads as follows (with $\Delta t (> 0)$ a time discretization step that we suppose constant, for simplicity):

$$u^0 = u_0; \quad (28)$$

then, for $n \geq 1$, compute u^n from u^{n-1} via the solution of

$$\begin{aligned} u^n &\in H_0^1(\Omega), \quad \rho \int_{\Omega} (u^n - u^{n-1})(v - u^n) dx + \mu \Delta t \int_{\Omega} \nabla u^n \cdot \nabla (v - u^n) dx + g \Delta t (j(v) - j(u^n)) \geq \Delta t C^n \int_{\Omega} (v - u^n) dx, \\ \forall v &\in H_0^1(\Omega), \end{aligned} \quad (29)$$

with $C^n = C(n \Delta t)$. It follows from, e.g., ([10], Chapter I) that (29) is an elliptic variational inequality (of the second kind) problem, which has a unique solution. Concerning schemes (28) and (29) we have the following stability.

Theorem 4. *Suppose that $C(t)$ is bounded on $(0, T)$ and that $u_0 \in L^2(\Omega)$; then the schemes (28) and (29) is unconditionally stable. Moreover, if the upper bound of $C(t)$ is small enough, there exists an integer $n_c \geq 0$, such that*

$$u^n = 0, \quad \forall n \geq n_c \quad (30)$$

Proof. Taking $v = 2u^n$ and 0 in the variational inequality in (29), we obtain, by comparison, the following relation

$$\rho \int_{\Omega} (u^n - u^{n-1})u^n dx + \mu \Delta t \int_{\Omega} |\nabla u^n|^2 dx + g \Delta t j(u^n) = C^n \Delta t \int_{\Omega} u^n dx. \quad (31)$$

Let us denote $\sup_{t \in (0, T)} |C(t)|$ by $\|C\|_{\infty}$. Using the Schwarz inequality in $L^2(\Omega)$ and the Strauss–Nirenberg inequality

$$\gamma \|v\|_{L^2(\Omega)} \leq j(v), \quad \forall v \in H_0^1(\Omega),$$

it follows from (31) that

$$\|u^n\|_{L^2(\Omega)}^2 - \|u^{n-1}\|_{L^2(\Omega)}^2 + \frac{2\mu \Delta t}{\rho} \|\nabla u^n\|_{L^2(\Omega)}^2 \leq \frac{2\Delta t}{\rho} (\|C\|_{\infty} |\Omega|^{1/2} - g\gamma)^+ \|u^n\|_{L^2(\Omega)}, \quad (32)$$

$\forall n \geq 1$, (where $z^+ = \max(0, z)$). If $g \geq \|C\|_\infty |\Omega|^{1/2} / \gamma$, relation (32) implies $\|u^n\|_{L^2(\Omega)} \leq \|u^0\|_{L^2(\Omega)}$, $\forall n \geq 1$, i.e., the unconditional stability of the scheme. Suppose now that $g < \|C\|_\infty |\Omega|^{1/2} / \gamma$ and denote by K the (positive) quantity $\|C\|_\infty |\Omega|^{1/2} - g\gamma$. Combining (32) and the relations

$$2ab \leq \alpha a^2 + \frac{b^2}{\alpha}, \quad \forall a, b \in \mathbb{R} \text{ and } \forall \alpha > 0,$$

$$\lambda_0 \|v\|_{L^2(\Omega)}^2 \leq \|\nabla v\|_{(L^2(\Omega))^2}^2, \quad \forall v \in H_0^1(\Omega) \text{ (Poincaré Inequality)},$$

where λ_0 is the smallest eigenvalue of the operator $-\nabla^2$ for the homogeneous Dirichlet boundary conditions, we obtain

$$\left(1 + \frac{\mu \Delta t}{\varrho} \lambda_0\right) \|u^n\|_{L^2(\Omega)}^2 \leq \frac{\Delta t K^2}{\varrho \lambda_0 \mu} + \|u^{n-1}\|_{L^2(\Omega)}^2, \quad \forall n \geq 1. \tag{33}$$

Let us denote by θ the quantity $1 + \mu \Delta t \lambda_0 / \varrho$; it follows from (33) that

$$\|u^n\|_{L^2(\Omega)}^2 \leq \frac{\Delta t K^2}{\varrho \lambda_0 \mu} \sum_{j=1}^n \theta^{-j} + \|u_0\|_{L^2(\Omega)}^2 \theta^{-n}, \quad \forall n \geq 1. \tag{34}$$

Since $\theta > 1$, (34) implies that

$$\|u^n\|_{L^2(\Omega)}^2 \leq \Delta t K^2 / \varrho \lambda_0 \mu \theta^{-1} / (1 - \theta^{-1}) + \|u_0\|_{L^2(\Omega)}^2, \quad \forall n \geq 1,$$

a relation which implies in turn (since $\frac{\theta^{-1}}{1-\theta^{-1}} = \frac{1}{\theta-1}$) that

$$\|u^n\|_{L^2(\Omega)}^2 \leq (\lambda_0 \mu)^{-2} K^2 + \|u_0\|_{L^2(\Omega)}^2, \quad \forall n \geq 1, \tag{35}$$

i.e., the unconditional stability of schemes (28) and (29) when $g < \|C\|_\infty |\Omega|^{1/2} / \gamma$.

To complete the proof of the theorem, we still have to show that property (30) holds if $C(t)$ is sufficiently small. Suppose indeed that

$$\|C\|_\infty < \gamma g |\Omega|^{-1/2}, \tag{36}$$

it follows from (31), and from the various inequalities already used above, that

$$\varrho (\|u^n\|_{L^2(\Omega)} - \|u^{n-1}\|_{L^2(\Omega)}) \|u^n\|_{L^2(\Omega)} + \Delta t \lambda_0 \mu \|u^n\|_{L^2(\Omega)}^2 + \Delta t (g\gamma - \|C\|_\infty |\Omega|^{1/2}) \|u^n\|_{L^2(\Omega)} \leq 0, \quad \forall n \geq 1. \tag{37}$$

Since (from (36)) $g\gamma - \|C\|_\infty |\Omega|^{1/2} > 0$, it follows from (37) that if there exists n_0 such that $u^{n_0} = 0$, then $u^n = 0$, $\forall n \geq n_0$. Suppose now that $u^n \neq 0$, $\forall n \geq 0$. We have then, from (37),

$$(\|u^n\|_{L^2(\Omega)} - \|u^{n-1}\|_{L^2(\Omega)}) + \frac{\Delta t}{\varrho} \lambda_0 \mu \|u^n\|_{L^2(\Omega)} + \frac{\Delta t}{\varrho} (g\gamma - \|C\|_\infty |\Omega|^{1/2}) \leq 0, \quad \forall n \geq 1 \tag{38}$$

Relation (38) can be rewritten as

$$(\|u^n\|_{L^2(\Omega)} - \|u^{n-1}\|_{L^2(\Omega)}) + \frac{\Delta t}{\varrho} \lambda_0 \mu \left[\|u^n\|_{L^2(\Omega)} + (\lambda_0 \mu)^{-1} (g\gamma - \|C\|_\infty |\Omega|^{1/2}) \right] \leq 0, \tag{39}$$

$\forall n \geq 1$. Introduce now $y^n = \|u^n\|_{L^2(\Omega)} + (\lambda_0 \mu)^{-1} (g\gamma - \|C\|_\infty |\Omega|^{1/2})$; it follows from (39) that

$$(1 + \Delta t \varrho^{-1} \lambda_0 \mu) y^n \leq y^{n-1}, \quad \forall n \geq 1,$$

which implies that

$$y^n \leq (1 + \Delta t \varrho^{-1} \lambda_0 \mu)^{-n} y_0. \tag{40}$$

Relation (40) implies that $\lim_{n \rightarrow +\infty} y^n = 0$, i.e., $\lim_{n \rightarrow +\infty} [\|u^n\|_{L^2(\Omega)} + (\lambda_0 \mu)^{-1} (g\gamma - \|C\|_\infty |\Omega|^{1/2})] = 0$, which is impossible since $g\gamma - \|C\|_\infty |\Omega|^{1/2} > 0$. There exists thus an index n_c such that (30) holds; this completes the proof of the theorem. \square

Remark 5. From relation (40) we can derive an upper bound for the above index n_c . Indeed, it follows from the definition of y^n that (40) can not hold for those n verifying

$$n \geq \frac{\ln[1 + \lambda_0 \mu \|u_0\|_{L^2(\Omega)} / (g\gamma - \|C\|_\infty |\Omega|^{1/2})]}{\ln(1 + \Delta t \varrho^{-1} \lambda_0 \mu)}, \tag{41}$$

implying that the corresponding $u^n = 0$. Assuming that $\{u^n\}_{n \geq 0}$ converges in some sense to the solution u of the continuous problem (17), when $\Delta t \rightarrow 0$ (a result not too difficult to prove), we observe (after multiplying both sides of the inequality (41) by Δt) that

$$u(t) = 0, \quad \forall t \geq \frac{\varrho}{\lambda_0 \mu} \ln \left[1 + \frac{\lambda_0 \mu \|u_0\|_{L^2(\Omega)}}{(g\gamma - \|C\|_\infty |\Omega|^{1/2})} \right]. \quad (42)$$

Relation (42) is consistent with the “cut-off” relations (21) and (22). To the best of our knowledge, the backward Euler scheme is the only time-discretization scheme to enjoy these asymptotic properties, mimicking those of the continuous model.

Remark 6. Concerning the solution of problem (17), there are many situations of practical interest where $u(t)$ does not have the $C^2(\bar{\Omega})$ -regularity and where, moreover, $u \notin C^1([0, T]; L^2(\Omega))$. This lack of regularity, with respect to both the space and time variables, suggests that there are little advantages at using approximations of higher order than backward Euler for the time discretization and piecewise linear finite elements for the space one. The numerical experiments and comparisons reported in [13] validate these predictions; what was compared in [13] were computations based, on the one hand, on

$$u_h^0 = u_{0h} (\in V_h) \quad (43)$$

then, for $n \geq 1$, compute u_h^n from u_h^{n-1} via the solution of

$$\begin{aligned} u_h^n \in V_{0h}, \quad \varrho \int_{\Omega_h} (u_h^n - u_h^{n-1})(v - u_h^n) dx + \mu \Delta t \int_{\Omega_h} \nabla u_h^n \cdot \nabla (v - u_h^n) dx + g \Delta t (j_h(v) - j_h(u_h^n)) \\ \geq \Delta t C^n \int_{\Omega_h} (v - u_h^n) dx, \quad \forall v \in V_{0h}, \end{aligned} \quad (44)$$

and, on the other hand, on

$$u_h^0 = u_{0h} (\in V_{0h}); \quad (45)$$

then, compute first u_h^1 from

$$u_h^1 = 2u_h^{1/2} - u_h^0, \quad (46)$$

where, in (46), $u_h^{1/2}$ is the solution of

$$\begin{aligned} u_h^{1/2} \in V_{0h} \quad \varrho \int_{\Omega_h} (u_h^{1/2} - u_h^0)(v - u_h^{1/2}) dx + \frac{\mu \Delta t}{2} \int_{\Omega_h} \nabla u_h^{1/2} \cdot \nabla (v - u_h^{1/2}) dx + \frac{g \Delta t}{2} (j_h(v) - j_h(u_h^{1/2})) \\ \geq \frac{\Delta t C^{1/2}}{2} \int_{\Omega_h} (v - u_h^{1/2}) dx, \quad \forall v \in V_{0h}, \end{aligned} \quad (47)$$

and next, for $n \geq 2$, u_h^n is obtained via the solution of

$$\begin{aligned} u_h^n \in V_{0h}, \quad \varrho \int_{\Omega_h} (1.5u_h^n - 2u_h^{n-1} + 0.5u_h^{n-2})(v - u_h^n) dx + \mu \Delta t \int_{\Omega_h} \nabla u_h^n \cdot \nabla (v - u_h^n) dx + g \Delta t (j_h(v) - j_h(u_h^n)) \\ \geq \Delta t C^n \int_{\Omega_h} (v - u_h^n) dx, \quad \forall v \in V_{0h}. \end{aligned} \quad (48)$$

In Ref. [13], we had:

- In (43) and (44), the finite element spaces V_h and V_{0h} defined by

$$V_h = \{v | v \in C^0(\bar{\Omega}_h), v|_K \in P_1, \forall K \in \mathcal{T}_h\} \quad (49)$$

and

$$V_{0h} = \{v | v \in V_h, v = 0 \text{ on } \Gamma\}, \quad (50)$$

respectively, with \mathcal{T}_h a triangulation of Ω , $\bar{\Omega}_h = \bigcup_{K \in \mathcal{T}_h} K$ (assuming that the K are closed triangles), Ω_h the interior of $\bar{\Omega}_h$, and

P_1 the space of the polynomials in two variables of degree ≤ 1 .

- In (45)–(48), the finite element space V_{0h} defined by

$$V_{0h} = \{v | v \in C^0(\bar{\Omega}_h), v|_K \in P_2(K), \forall K \in \mathcal{T}_h, v = 0 \text{ on } \Gamma\}, \quad (51)$$

with \mathcal{T}_h a triangulation containing possibly curved triangles (to better follow the curved parts of the boundary, if such parts exist), $\bar{\Omega}_h = \bigcup_{K \in \mathcal{T}_h} K$, $\Omega_h =$ the interior of $\bar{\Omega}_h$, $P_2(K) = P_2$ if K is a rectilinear triangle and, if K is a curved triangle, $P_2(K)$ is obtained from P_2 via the quadratic mapping based isoparametric methodology discussed in, e.g., [14,15] and [7].

- $\lim_{h \rightarrow 0} u_{0h} = u_0$ in $L^2(\Omega)$.
- In (44),

$$j_h(v) = \sum_{K \in \mathcal{T}_h} \int_K |\nabla v| \, dx$$

while, in (45), $j_h(\cdot)$ is obtained from $\sum_{K \in \mathcal{T}_h} \int_K |\nabla v| \, dx$ using a Simpson rule related numerical integration method to compute the integrals over the triangles K .

Observe that the step (47) is of the Crank–Nicolson type, while the scheme used in (48) is fully implicit and two-step backward. Scheme (45)–(48) is second order accurate (when applied to the solution of smooth problems (which is not the case here)) and stiff A-stable (like schemes (43) and (44)). Other schemes are available.

It is worth mentioning that an adaptive finite element method for the solution of the steady-state variant of problem (17) is discussed in [16]; it relies on piecewise quadratic approximations similar to those in (51). Adaptivity provides here a way to overcome the low accuracy of the approximate solutions resulting from the lack of regularity of the solution (H^2 -regularity at most).

7. Bingham flow in cylinders. (V) Steady flow

7.1. Formulation of the problem. Synopsis

Suppose that the pressure drop C is independent of t . It follows then from, e.g., [10] that the steady state problem associated to (17), namely

$$u_\infty \in H_0^1(\Omega), \quad \mu \int_\Omega \nabla u_\infty \cdot \nabla(v - u_\infty) \, dx + g(j(v) - j(u_\infty)) \geq C \int_\Omega (v - u_\infty) \, dx, \quad \forall v \in H_0^1(\Omega), \tag{52}$$

has a unique solution. In order to solve (52) (an elliptic variational inequality problem), several approaches are available, several of them discussed in, e.g., Refs. [10–13]; among them

- (i) Solve the corresponding problem (17) on the time interval $(0, +\infty)$ until a steady state is reached.
- (ii) Apply to (52), directly, the “old-fashioned” Uzawa method (introduced, a very long time ago, in [17]).
- (iii) Use some of the time dependent methods advocated in [12] which provide short-cuts to u_∞ .
- (iv) Use augmented Lagrangian methods associated to the linear constraint $\mathbf{p} = \nabla u$ (this approach is increasingly popular and has been used in, e.g., [16] and [18–20], the last reference concerning the numerical simulation of Electro-Rheological fluid flow).

We will discuss below all the four above approaches, but also a recently introduced one, combining penalty techniques, the Newton’s method and conjugate gradient algorithms.

7.2. Computing u_∞ via the solution of the time dependent problem

Relation (23) in the statement of Theorem 2 (see Section 5), shows that integrating (17) from 0 to $+\infty$ provides u_∞ with exponential speed in $L^2(\Omega)$; actually, this property still holds if one applies the backward Euler scheme to the solution of problem (17). Let us prove this property: assuming that the pressure drop C is time independent, the backward Euler schemes (28) and (29) takes the following form:

$$u^0 = u_0; \tag{53}$$

then, for $n \geq 1$, compute u^n from u^{n-1} via the solution of

$$u^n \in H_0^1(\Omega), \quad \varrho \int_\Omega (u^n - u^{n-1})(v - u^n) \, dx + \mu \Delta t \int_\Omega \nabla u^n \cdot \nabla(v - u^n) \, dx + g \Delta t (j(v) - j(u^n)) \geq \Delta t C \int_\Omega (v - u^n) \, dx, \tag{54}$$

$$\forall v \in H_0^1(\Omega).$$

Denote $u^n - u_\infty$ by \bar{u}^n ; taking $v = u^n$ (resp., $v = u_\infty$) in (52) (resp., (54)) and adding (after multiplying by Δt both sides of the inequality in (52)), we obtain

$$\varrho \int_{\Omega} (\bar{u}^n - \bar{u}^{n-1}) \bar{u}^n \, dx + \mu \Delta t \|\nabla \bar{u}^n\|_{(L^2(\Omega))^2}^2 \leq 0, \quad \forall n \geq 1. \quad (55)$$

Combining (55) with the Schwarz inequality in $L^2(\Omega)$, and the Poincaré inequality in $H_0^1(\Omega)$, we obtain

$$\frac{\varrho}{2} (\|\bar{u}^n\|_{L^2(\Omega)}^2 - \|\bar{u}^{n-1}\|_{L^2(\Omega)}^2) + \mu \lambda_0 \Delta t \|\bar{u}^n\|_{L^2(\Omega)}^2 \leq 0, \quad \forall n \geq 1, \quad (56)$$

where λ_0 is the smallest eigenvalue of the operator $-\nabla^2$ for the homogeneous Dirichlet boundary conditions. It follows from (56) that

$$(1 + 2\mu\lambda_0\varrho^{-1}\Delta t)\|\bar{u}^n\|_{L^2(\Omega)}^2 \leq \|\bar{u}^{n-1}\|_{L^2(\Omega)}^2, \quad \forall n \geq 1,$$

which implies in turn that

$$\|\bar{u}^n\|_{L^2(\Omega)} \leq (1 + 2\mu\lambda_0\varrho^{-1}\Delta t)^{-n/2} \|\bar{u}^0\|_{L^2(\Omega)}, \quad n \geq 0. \quad (57)$$

The exponential convergence (in $L^2(\Omega)$) of u^n to u_∞ follows from (57). Actually, relation (57) still holds if one replaces (52), (53), and (54) by their finite element analogues.

Of course, when applying the fully implicit schemes (53) and (54) to the computation of u_∞ we still have to address the solution of the elliptic variational inequalities (54); this important issue will be discussed in the following section.

7.3. An iterative method à la Uzawa for the solution of problems (52) and (54)

Both problems (49) and (51) are particular cases of

$$u \in H_0^1(\Omega), \quad \alpha \int_{\Omega} u(v-u) \, dx + \mu \int_{\Omega} \nabla u \cdot \nabla(v-u) \, dx + g(j(v) - j(u)) \geq \int_{\Omega} f(v-u) \, dx, \quad \forall v \in H_0^1(\Omega), \quad (58)$$

with $\alpha \geq 0$ and $f \in L^2(\Omega)$.

A classical method to solve problem (58) is the one introduced in Ref. [17]; it reduces the solution of the above problem to the solution of a sequence of linear Dirichlet problems for the operator $\alpha\mathbf{I} - \mu\nabla^2$ and simple projection operations. The method relies on the equivalence between (58) and

$$\alpha u - \mu \nabla^2 u - g \nabla \cdot \boldsymbol{\lambda} = f \text{ in } \Omega, \quad u = 0 \text{ on } \Gamma, \quad \boldsymbol{\lambda} \cdot \nabla u = |\nabla u|, \quad \boldsymbol{\lambda} \in \boldsymbol{\Lambda}, \quad (59)$$

the last two relations implying that

$$\boldsymbol{\lambda} = P_{\boldsymbol{\Lambda}}(\boldsymbol{\lambda} + rg \nabla u), \quad \forall r \geq 0, \quad (60)$$

with the operator $P_{\boldsymbol{\Lambda}}$ defined by (27).

In order to solve (58), via relations (59) and (60), we advocate (following [17]) the fixed point algorithm below:

$$\boldsymbol{\lambda}^0 \text{ is given in } \boldsymbol{\Lambda} \quad (61)$$

then, for $n \geq 0$, assuming that $\boldsymbol{\lambda}^n$ is known, we compute u^n and then $\boldsymbol{\lambda}^{n+1}$ as follows:

solve

$$\alpha u^n - \mu \nabla^2 u^n = f + g \nabla \cdot \boldsymbol{\lambda}^n \text{ in } \Omega, \quad u^n = 0 \text{ on } \Gamma, \quad (62)$$

and

$$\boldsymbol{\lambda}^{n+1} = P_{\boldsymbol{\Lambda}}(\boldsymbol{\lambda}^n + rg \nabla u^n). \quad (63)$$

Remark 7. Suppose that the system (59) has a solution $\{u, \boldsymbol{\lambda}\} \in H_0^1(\Omega) \times \boldsymbol{\Lambda}$ (which is indeed the case); it can be shown (see, e.g., Refs. [10,11]) that the above pair is necessarily a saddle-point over $H_0^1(\Omega) \times \boldsymbol{\Lambda}$ of the Lagrangian functional

$$\mathcal{L} : H^1(\Omega) \times (L^2(\Omega))^2 \rightarrow \mathbb{R}$$

defined by

$$\mathcal{L}(v, \boldsymbol{\mu}) = \frac{1}{2} \left[\alpha \|v\|_{L^2(\Omega)}^2 + \mu \|\nabla v\|_{(L^2(\Omega))^2}^2 \right] + g \int_{\Omega} \boldsymbol{\mu} \cdot \nabla v \, dx - \int_{\Omega} f v \, dx \quad (64)$$

i.e., the pair $\{u, \boldsymbol{\lambda}\}$ verifies (from the definition of a saddle-point; see, e.g., ([7], Chapter 4))

$$\{u, \boldsymbol{\lambda}\} \in H_0^1(\Omega) \times \boldsymbol{\Lambda}, \quad \mathcal{L}(u, \boldsymbol{\mu}) \leq \mathcal{L}(u, \boldsymbol{\lambda}) \leq \mathcal{L}(v, \boldsymbol{\lambda}), \quad \forall \{v, \boldsymbol{\mu}\} \in H_0^1(\Omega) \times \boldsymbol{\Lambda}. \quad (65)$$

Conversely, any solution of (65) is solution of system (59). It follows from the above reference that algorithm (61)–(63) is nothing but an Uzawa algorithm applied to the solution of the saddle-point problem (65) with $\mathcal{L}(\cdot, \cdot)$ defined by (64); for a systematic study of Uzawa algorithms, see, e.g., ([7], Chapter 4) and the references therein.

Proving the convergence of algorithm (61)–(63) (for $r > 0$ and sufficiently small) is a relatively simple exercise; owing to the importance of these topics (in order to investigate, in the following sections, the convergence of variants of algorithm (61)–(63)) we feel compelled to give a proof of the convergence of the above algorithm. We have thus the following convergence

Theorem 5. *Suppose that*

$$0 < r < \frac{2\mu}{g^2}, \tag{66}$$

in (63). Then, $\forall \lambda^0 \in \Lambda$, the sequence $\{u^n, \lambda^n\}_{n \geq 0}$ generated by algorithm (61)–(63) verifies

$$\lim_{n \rightarrow +\infty} \{u^n, \lambda^n\} = \{u, \lambda^*\} \text{ in } H_0^1(\Omega) \times ((L^\infty(\Omega))^2 \text{ weak}^*), \tag{67}$$

where $\{u, \lambda^*\}$ is a solution of (59) in $H_0^1(\Omega) \times \Lambda$.

Proof. Let $\{u, \lambda\}$ be a solution of (59) in $H_0^1(\Omega) \times \Lambda$ and let us denote $u^n - u$ and $\lambda^n - \lambda$ by \bar{u}^n and $\bar{\lambda}^n$, respectively. Taking into account the fact that the operator P_Λ is a contraction of $(L^2(\Omega))^2$, we obtain by subtraction between (59), (60) and (62), (63) that, $\forall n \geq 0$,

$$\alpha \bar{u}^n - \mu \nabla^2 \bar{u}^n = g \nabla \cdot \bar{\lambda}^n \text{ in } \Omega, \quad \bar{u}^n = 0 \text{ on } \Gamma, \quad \|\bar{\lambda}^{n+1}\|_{(L^2(\Omega))^2} \leq \|\bar{\lambda}^n + rg \nabla \bar{u}^n\|_{(L^2(\Omega))^2}. \tag{68}$$

It follows then from the third relation (68) that

$$\|\bar{\lambda}^{n+1}\|_{(L^2(\Omega))^2}^2 \leq \|\bar{\lambda}^n\|_{(L^2(\Omega))^2}^2 + 2rg \int_{\Omega} \bar{\lambda}^n \cdot \nabla \bar{u}^n \, dx + r^2 g^2 \|\nabla \bar{u}^n\|_{(L^2(\Omega))^2}^2,$$

which implies in turn

$$\|\bar{\lambda}^n\|_{(L^2(\Omega))^2}^2 - \|\bar{\lambda}^{n+1}\|_{(L^2(\Omega))^2}^2 \geq -2rg \int_{\Omega} \bar{\lambda}^n \cdot \nabla \bar{u}^n \, dx - r^2 g^2 \|\nabla \bar{u}^n\|_{(L^2(\Omega))^2}^2. \tag{69}$$

We observe, next, that, after integration by parts, the first two relations in (68) imply that

$$\alpha \|\bar{u}^n\|_{L^2(\Omega)}^2 + \mu \|\nabla \bar{u}^n\|_{(L^2(\Omega))^2}^2 = -g \int_{\Omega} \bar{\lambda}^n \cdot \nabla \bar{u}^n \, dx. \tag{70}$$

Combining relations (69) and (70), we obtain

$$\begin{aligned} \|\bar{\lambda}^n\|_{(L^2(\Omega))^2}^2 - \|\bar{\lambda}^{n+1}\|_{(L^2(\Omega))^2}^2 &\geq 2r \left[\alpha \|\bar{u}^n\|_{L^2(\Omega)}^2 + \mu \|\nabla \bar{u}^n\|_{(L^2(\Omega))^2}^2 \right] - r^2 g^2 \|\nabla \bar{u}^n\|_{(L^2(\Omega))^2}^2 \\ &\geq r \left(2 - \frac{rg^2}{\mu} \right) \left[\alpha \|\bar{u}^n\|_{L^2(\Omega)}^2 + \mu \|\nabla \bar{u}^n\|_{(L^2(\Omega))^2}^2 \right]. \end{aligned} \tag{71}$$

Suppose that the condition (66) holds; it implies that $r(2 - rg^2/\mu) > 0$. It follows then from (71) that the sequence $\left\{ \|\bar{\lambda}^n\|_{(L^2(\Omega))^2}^2 \right\}_{n \geq 0}$ is decreasing; this sequence being bounded from below by 0 is converging to some (nonnegative) limit, which implies that

$$\lim_{n \rightarrow +\infty} (\|\bar{\lambda}^n\|_{L^2(\Omega)}^2 - \|\bar{\lambda}^{n+1}\|_{L^2(\Omega)}^2) = 0. \tag{72}$$

Combining (71) and (72) we obtain $\lim_{n \rightarrow +\infty} \bar{u}^n$ in $H_0^1(\Omega)$, namely the convergence of $\{u^n\}_{n \geq 0}$ to u in $H_0^1(\Omega)$. Proving the convergence of $\{\lambda^n\}_{n \geq 0}$ is a more complicated issue that we will not address here (it is discussed in, e.g., ([7], Chapter 4) and [11]). \square

Remark 8. All the solutions of system (59) share the same u . Suppose now that $\{u, \lambda\}$ and $\{u, \lambda'\}$ are solutions of (59); we have then

$$\nabla \cdot (\lambda' - \lambda) = 0. \tag{73}$$

Keeping in mind that

$$(L^2(\Omega))^2 = \nabla H_0^1(\Omega) \oplus \mathbf{S}_0, \tag{74}$$

where $\mathbf{S}_0 = \{\mathbf{q} | \mathbf{q} \in (L^2(\Omega))^2, \nabla \cdot \mathbf{q} = 0\}$, it follows from (73), that all the pairs $\{u, \lambda\}$, solutions of (59), not only share the same argument u , but all the λ s have the same component in $\nabla H_0^1(\Omega)$ when decomposed according to (74). Another consequence is the following.

Consider $\mathbf{q} \in (L^2(\Omega))^2$; it follows from (74) that $\mathbf{q} = \mathbf{q}_1 + \mathbf{q}_2$, with $\mathbf{q}_1 \in \nabla H_0^1(\Omega)$ and $\mathbf{q}_2 \in \mathbf{S}_0$, respectively, the above decomposition being unique. If $\{u, \lambda\}$ is solution of (59), all the λ s have λ_1 in common in the decomposition (74) of $(L^2(\Omega))^2$. Suppose now that r verifies the condition (66); it follows then from Theorem 5 and from (68), (74) that

$$\lim_{n \rightarrow +\infty} \lambda_1^n = \lambda_1 \text{ in } (L^2(\Omega))^2. \quad (75)$$

The frequently observed slow convergence of algorithm (61)–(63), particularly when g is large, seems to be related to the relative importance of λ_2 compared to λ_1 . The more important λ_2 , the slower is the convergence, everything else being the same.

Remark 9. By formal elimination of u in (59) we can show that in fact λ is solution of a kind of elliptic variational inequality of the obstacle type. To show that, we observe first that any pair $\{u, \lambda\}$ solution of (59) in $H_0^1(\Omega) \times \mathbf{\Lambda}$ verifies

$$\lambda \in \mathbf{\Lambda}, \quad \int_{\Omega} (-\nabla u) \cdot (\mu - \lambda) dx \geq 0, \quad \forall \mu \in \mathbf{\Lambda}, \quad \alpha u - \mu \nabla^2 u = f + g \nabla \cdot \lambda \text{ in } \Omega, \quad u = 0 \text{ on } \Gamma. \quad (76)$$

Next, we introduce the continuous and linear operator \mathbf{A} from $(L^2(\Omega))^2$ into $(L^2(\Omega))^2$, defined as follows:

$$\mathbf{A}\mathbf{q} = -\nabla u_{\mathbf{q}}, \quad \forall \mathbf{q} \in (L^2(\Omega))^2, \quad (77)$$

where $u_{\mathbf{q}}$ is the unique solution in $H_0^1(\Omega)$ of the Dirichlet problem

$$\alpha u_{\mathbf{q}} - \mu \nabla^2 u_{\mathbf{q}} = g \nabla \cdot \mathbf{q}, \quad \text{in } \Omega, \quad u_{\mathbf{q}} = 0 \text{ on } \Gamma. \quad (78)$$

We have, $\forall \mathbf{q}, \mathbf{q}' \in (L^2(\Omega))^2$,

$$\int_{\Omega} (\mathbf{A}\mathbf{q}) \cdot \mathbf{q}' dx = - \int_{\Omega} \nabla u_{\mathbf{q}} \cdot \mathbf{q}' dx = \langle u_{\mathbf{q}}, \nabla \cdot \mathbf{q}' \rangle = \frac{1}{g} \langle u_{\mathbf{q}}, \alpha u_{\mathbf{q}'} - \mu \nabla^2 u_{\mathbf{q}'} \rangle = \frac{1}{g} \int_{\Omega} [\alpha u_{\mathbf{q}} u_{\mathbf{q}'} + \mu \nabla u_{\mathbf{q}} \cdot \nabla u_{\mathbf{q}'}] dx, \quad (79)$$

where in (79), $\langle \cdot, \cdot \rangle$ denotes the pairing between $H_0^1(\Omega)$ and its dual space $H^{-1}(\Omega)$. It follows from (79) that operator \mathbf{A} is symmetric and positive semi-definite; \mathbf{A} is not positive definite since we clearly have $\text{Ker}(\mathbf{A}) = \mathbf{S}_0$, with \mathbf{S}_0 as in (74). Finally, define u_f as the unique solution in $H_0^1(\Omega)$ of the following Dirichlet problem

$$\alpha u_f - \mu \nabla^2 u_f = f \text{ in } \Omega, \quad u_f = 0 \text{ on } \Gamma \quad (80)$$

(if Γ is smooth enough and/or Ω is convex, then $u_f \in H_0^1(\Omega) \cap H^2(\Omega)$, implying that $\nabla u_f \in (H^1(\Omega))^2 \subset (L^s(\Omega))^2, \forall s \in [1, +\infty)$). It follows then from (76)–(78) that

$$\nabla u = \nabla u_f + \nabla u_{\lambda} = \nabla u_f - \mathbf{A}\lambda,$$

which combined with (76) implies that the vector-valued function λ is a solution of the following “elliptic” variational inequality (in the sense of Lions and Stampacchia (Ref. [21])):

$$\lambda \in \mathbf{\Lambda}, \quad \int_{\Omega} \mathbf{A}\lambda \cdot (\mu - \lambda) dx \geq \int_{\Omega} \nabla u_f \cdot (\mu - \lambda) dx, \quad \forall \mu \in \mathbf{\Lambda}, \quad (81)$$

which, from the very nature of the convex set $\mathbf{\Lambda}$, is definitely an obstacle problem. Incidentally, an equivalent formulation of algorithm (61)–(63) is given by

$$\lambda^0 \text{ is given in } \mathbf{\Lambda}; \quad (82)$$

then, for $n \geq 0$, assuming that λ^n is known, compute λ^{n+1} as follows:

solve

$$\lambda^{n+1} = P_{\mathbf{\Lambda}}[\lambda^n - rg(\mathbf{A}\lambda^n - \nabla u_f)], \quad (83)$$

implying that the above algorithm is (from the symmetry of operator \mathbf{A}) a gradient method with projection.

Two other iterative methods for the solution of problem (58), (59) will be discussed in the following sections; more method are discussed in Ref. [12].

7.4. A (pseudo-) time relaxation approach for the solution of problem (58), (59)

To the best of our knowledge the method to be discussed now is new; in fact it improves on related methods discussed in Ref. [11] and has some similarities with methods recently introduced in Image Processing. The basic idea is pretty simple and quite general: it consists in associating with (58) and (59) a well-chosen dynamical system (initial value problem) that we integrate from 0 to $+\infty$

in order to capture the related steady state solutions, if such solutions exist, which is the case here. The initial value problem that we consider is the dynamical variant of problem (81) defined as follows (with τ a pseudo-time):

$$\lambda(0) = \lambda_0 (\in \Lambda); \tag{84}$$

$$\lambda(\tau) \in \Lambda, \quad \tau \in [0, +\infty), \quad \int_{\Omega} (\partial_{\tau} \lambda + g \mathbf{A} \lambda) \cdot (\mu - \lambda) \, dx \geq g \int_{\Omega} \nabla u_f \cdot (\mu - \lambda) \, dx, \quad \forall \mu \in \Lambda. \tag{85}$$

An equivalent, but more explicit formulation of the initial value problems (84) and (85) is given by replacing (85) by

$$\alpha u - \mu \nabla^2 u - g \nabla \cdot \lambda = f \text{ in } \Omega, \quad u = 0 \text{ on } \Gamma, \quad \lambda(\tau) \in \Lambda, \quad \tau \in [0, +\infty), \quad \int_{\Omega} (\partial_{\tau} \lambda - g \nabla u) \cdot (\mu - \lambda) \, dx \geq 0, \quad \forall \mu \in \Lambda. \tag{86}$$

To time-discretize problems (85) and (86) we advocate the following backward Euler scheme

$$\lambda^0 = \lambda_0; \tag{87}$$

then, for $n \geq 1$, compute λ^n from λ^{n-1} via the solution of

$$\alpha u^n - \mu \nabla^2 u^n - g \nabla \cdot \lambda^n = f \text{ in } \Omega, \quad u^n = 0 \text{ on } \Gamma, \quad \lambda^n \in \Lambda, \quad \int_{\Omega} \left[\frac{(\lambda^n - \lambda^{n-1})}{\Delta \tau} - g \nabla u^n \right] \cdot (\mu - \lambda^n) \, dx \geq 0, \quad \forall \mu \in \Lambda, \tag{88}$$

with $\Delta \tau (> 0)$ a (pseudo-) time discretization step. From the properties of operator \mathbf{A} , problem (88) has a unique solution. In order to solve system (88), we observe first that the vector-valued function λ^n verifies

$$\lambda^n \in \Lambda, \quad \int_{\Omega} \left[\lambda^n + r \frac{(\lambda^{n-1} - \lambda^n)}{\Delta \tau} + r g \nabla u^n - \lambda^n \right] \cdot (\mu - \lambda^n) \, dx \leq 0, \quad \forall \mu \in \Lambda, \quad \forall r > 0,$$

which makes (88) equivalent to

$$\lambda^n = P_{\Lambda} \left[\lambda^n + r \frac{(\lambda^{n-1} - \lambda^n)}{\Delta \tau} + r g \nabla u^n \right], \quad \forall r > 0. \tag{89}$$

To compute $\{u^n, \lambda^n\}$ we suggest the following fixed point algorithm:

$$\lambda_0^n \text{ is given in } \Lambda \text{ (a most natural choice being } \lambda_0^n = \lambda^{n-1}); \tag{90}$$

for $k \geq 0$, λ_k^n being known, compute u_k^n and λ_{k+1}^n as follows:

Solve first

$$\alpha u_k^n - \mu \nabla^2 u_k^n = f + g \nabla \cdot \lambda_k^n \text{ in } \Omega, \quad u_k^n = 0 \text{ on } \Gamma, \tag{91}$$

and update λ_k^n via

$$\lambda_{k+1}^n = P_{\Lambda} \left[\lambda_k^n + r \frac{(\lambda^{n-1} - \lambda_k^n)}{\Delta \tau} + r g \nabla u_k^n \right]. \tag{92}$$

Concerning the convergence of algorithm (90)–(92) to the unique solution of system (88) in $H_0^1(\Omega) \times (L^2(\Omega))^2$, we have the following

Theorem 6. *Suppose that*

$$0 < r \leq \frac{2\mu}{2\mu + g^2 \Delta \tau} \Delta \tau; \tag{93}$$

we have then, $\forall \lambda_0^n$ in (90),

$$\lim_{k \rightarrow +\infty} \{u_k^n, \lambda_k^n\} = \{u^n, \lambda^n\} \text{ in } H_0^1(\Omega) \times (L^2(\Omega))^2, \tag{94}$$

the convergence being geometric.

Proof. We proceed as in the proof of Theorem 5. Denoting thus $u_k^n - u^n$ and $\lambda_k^n - \lambda^n$ by \bar{u}_k^n and $\bar{\lambda}_k^n$, respectively, we obtain by subtraction between (89) and (91), (92) that, $\forall k \geq 0$,

$$\alpha \bar{u}_k^n - \mu \nabla^2 \bar{u}_k^n = g \nabla \cdot \bar{\lambda}_k^n \text{ in } \Omega, \quad \bar{u}_k^n = 0 \text{ on } \Gamma, \tag{95}$$

and (from the contraction properties of operator P_{Λ})

$$\|\bar{\lambda}_{k+1}^n\|_{(L^2(\Omega))^2} \leq \left\| \left(1 - \frac{r}{\Delta\tau}\right) \bar{\lambda}_k^n + rg\nabla\bar{u}_k^n \right\|_{(L^2(\Omega))^2}. \quad (96)$$

Combining relations (95) and (96) yields

$$\|\bar{\lambda}_{k+1}^n\|_{(L^2(\Omega))^2}^2 + r \left[2\mu - r \left(\frac{2\mu}{\Delta\tau} + g^2 \right) \right] \|\nabla\bar{u}_k^n\|_{(L^2(\Omega))^2}^2 \leq \left(1 - \frac{r}{\Delta\tau}\right)^2 \|\bar{\lambda}_k^n\|_{(L^2(\Omega))^2}^2. \quad (97)$$

It follows from (97) that the convergence property (94) will take place if r verifies $|1 - r/\Delta\tau| < 1$ and $r[2\mu - r(2\mu/\Delta\tau + g^2)] \geq 0$, i.e., $0 < r < 2\Delta\tau$ and $r \leq 2\mu\Delta\tau/(2\mu + g^2\Delta\tau)$, respectively. Since $2\mu\Delta\tau/(2\mu + g^2\Delta\tau) < \Delta\tau < 2\Delta\tau$, condition (93) implies, clearly, the convergence property (94); indeed, we have more since the above discussion shows the existence of a constant K such that

$$\|u_k^n - u^n\|_{H_0^1(\Omega)} \leq K\|\lambda^n - \lambda_0^n\|_{(L^2(\Omega))^2} \left|1 - \frac{r}{\Delta\tau}\right|^k, \quad \forall k \geq 0, \quad \|\lambda_k^n - \lambda^n\|_{(L^2(\Omega))^2} \leq K\|\lambda^n - \lambda_0^n\|_{(L^2(\Omega))^2} \left|1 - \frac{r}{\Delta\tau}\right|^k, \quad (98)$$

which completes the proof of the theorem. \square

Remark 10. If one takes $\Delta\tau = 2\mu/g^2$ and $r = \Delta\tau/2 (= \mu/g^2)$ the convergence condition (93) is verified, the contraction factor in both relations (98) being $1/2$.

7.5. A penalty-Newton-Uzawa-conjugate gradient method for the solution of problem (58), (59)

The dual problem (81) is essentially (see Section 7.3) an obstacle problem associated to the point-wise constraint

$$|\lambda(x)| \leq 1, \quad \text{a.e. on } \Omega. \quad (99)$$

An alternative to the projection methods discussed so far is provided by a variant of the penalty-Newton-conjugate gradient method, applied in Refs. [22–24] to the solution of time dependent parabolic variational inequalities of the obstacle type. Let ε be a small positive parameter; we approximate the dual problem (81) by the following one:

$$\mathbf{A}\lambda_\varepsilon + \frac{1}{\varepsilon}(|\lambda_\varepsilon|^2 - 1)^+ \lambda_\varepsilon = \nabla u_f, \quad (100)$$

with $\xi^+ = \max(0, \xi)$, $\forall \xi \in \mathbb{R}$. The nonlinearity in (100) is reminiscent of a Ginzburg–Landau one. Using convexity/monotonicity arguments, and the fact that (100) is the Euler–Lagrange equation of the following problem from Calculus of Variations

$$\lambda_\varepsilon \in (L^6(\Omega))^2, \quad j_\varepsilon(\lambda_\varepsilon) \leq j_\varepsilon(\mu), \quad \forall \mu \in (L^6(\Omega))^2, \quad (101)$$

with

$$j_\varepsilon(\mu) = \frac{1}{2} \int_{\Omega} \mathbf{A}\mu \cdot \mu \, dx + \frac{1}{6\varepsilon} \int_{\Omega} (|\mu|^2 - 1)^+ dx - \int_{\Omega} \nabla u_f \cdot \mu \, dx,$$

we can easily prove that problems (100) and (101) has a solution in $(L^6(\Omega))^2$. From the definition of operator \mathbf{A} , problem (100) is equivalent to the following nonlinear system

$$\alpha u_\varepsilon - \mu \nabla^2 u_\varepsilon - g \nabla \cdot \lambda_\varepsilon = f \text{ in } \Omega, \quad u_\varepsilon = 0 \text{ on } \Gamma, \quad -\nabla u_\varepsilon + \frac{1}{\varepsilon}(|\lambda_\varepsilon|^2 - 1)^+ \lambda_\varepsilon = \mathbf{0} \quad (102)$$

(easier to handle than (100), in practice). Using relatively simple variants of the methods discussed in [10] (concerning the approximation of elliptic variational inequality problems), we can prove the following convergence properties

$$\lim_{\varepsilon \rightarrow 0} u_\varepsilon = u \text{ in } H_0^1(\Omega), \quad \lim_{\varepsilon \rightarrow 0} \lambda_\varepsilon = \lambda \text{ weakly in } (L^6(\Omega))^2, \quad (103)$$

where the pair $\{u, \lambda\}$ is a solution of problem (59) (implying in turn that λ is a solution of the obstacle problem (81)). Having thus justified the introduction of the approximate (by penalization) problem (100), we still have to address its solution. The Newton's method is an obvious candidate to achieve such a task; this leads to the following algorithm (after multiplying by ε both sides of (100) and dropping the subscripts ε):

$$\lambda^0 \text{ is given in } (L^6(\Omega))^2 (\lambda^0 = \mathbf{0}, \text{ for example}); \quad (104)$$

for $n \geq 0$, compute λ^{n+1} from λ^n via

$$\lambda^{n+1} = \lambda^n + \delta \lambda^n, \quad (105)$$

where, in (105), $\delta\lambda^n$ is solution of the following linear problem

$$\varepsilon\mathbf{A}\delta\lambda^n + (|\lambda^n|^2 - 1)^{+2}\delta\lambda^n + 4(|\lambda^n|^2 - 1)^+\lambda^n(\lambda^n \cdot \delta\lambda^n) = -[\varepsilon(\mathbf{A}\lambda^n - \nabla u_f) + (|\lambda^n|^2 - 1)^{+2}\lambda^n]; \quad (106)$$

we stop iterating when, typically, $\|\delta\lambda^n\|_{(L^2(\Omega))^2} \leq \text{tol}_1$.

The linear operator in the left-hand side of (106) is clearly symmetric and positive semi-definite; these properties suggest solving (106) by a conjugate gradient algorithm. From a practical point of view, it is preferable to consider directly the equivalent system (102); we are going to solve it by a Newton algorithm operating in $H_0^1(\Omega) \times (L^6(\Omega))^2$; this algorithm (equivalent to (104)–(106)) reads as follows:

$$\lambda^0 \text{ being given in } (L^6(\Omega))^2 (\lambda^0 = \mathbf{0}, \text{ for example}), \text{ solve } \alpha u^0 - \mu \nabla^2 u^0 = g \nabla \cdot \lambda^0 + f \text{ in } \Omega, \quad u^0 = 0 \text{ on } \Gamma \quad (107)$$

(the above elliptic problem has a unique solution in $H_0^1(\Omega)$ (in fact in $W_0^{1,6}(\Omega)$).

Then, for $n \geq 0$, compute $\{u^{n+1}, \lambda^{n+1}\}$ from $\{u^n, \lambda^n\}$ via

$$\{u^{n+1}, \lambda^{n+1}\} = \{u^n + \delta u^n, \lambda^n + \delta \lambda^n\}, \quad (108)$$

where, in (108), $\{\delta u^n, \delta \lambda^n\}$ is solution of

$$\alpha \delta u^n - \mu \nabla^2 \delta u^n - g \nabla \cdot \delta \lambda^n = 0 \text{ in } \Omega, \quad \delta u^n = 0 \text{ on } \Gamma, \quad (109)$$

$$-\varepsilon \nabla \delta u^n + (|\lambda^n|^2 - 1)^{+2} \delta \lambda^n + 4(|\lambda^n|^2 - 1)^+ \lambda^n (\lambda^n \cdot \delta \lambda^n) = \varepsilon \nabla u^n - (|\lambda^n|^2 - 1)^{+2} \lambda^n. \quad (110)$$

We are going to discuss now the solution of system (109), (110) by an Uzawa-conjugate gradient algorithm operating in the Hilbert space $H_0^1(\Omega) \times (L^2(\Omega))^2$. To further simplify the notation we denote δu^n by ψ , $\delta \lambda^n$ by \mathbf{p} , and by \mathbf{Q} the space $(L^2(\Omega))^2$; problems (109) and (110) takes then the following form:

$$\alpha \psi - \mu \nabla^2 \psi = g \nabla \cdot \mathbf{p} \text{ in } \Omega, \quad \psi = 0 \text{ on } \Gamma, \quad (111)$$

$$-\varepsilon \nabla \psi + (|\lambda^n|^2 - 1)^{+2} \mathbf{p} + 4(|\lambda^n|^2 - 1)^+ \lambda^n (\lambda^n \cdot \mathbf{p}) = \varepsilon \nabla u^n - (|\lambda^n|^2 - 1)^{+2} \lambda^n, \quad (112)$$

leading to the following algorithm:

Step 0. Initialization

$$\mathbf{p}^0 \text{ is given in } \mathbf{Q} (\mathbf{p}^0 = \mathbf{0} \text{ is a natural choice here}); \quad (113)$$

solve the following Dirichlet problem

$$\psi^0 \in H_0^1(\Omega), \quad \alpha \int_{\Omega} \psi^0 \varphi \, dx + \mu \int_{\Omega} \nabla \psi^0 \cdot \nabla \varphi \, dx = -g \int_{\Omega} \mathbf{p}^0 \cdot \nabla \varphi \, dx, \quad \forall \varphi \in H_0^1(\Omega), \quad (114)$$

and then

$$\begin{aligned} \mathbf{g}^0 \in \mathbf{Q}, \quad \int_{\Omega} \mathbf{g}^0 \cdot \mathbf{q} \, dx &= -\varepsilon \int_{\Omega} \nabla(\psi^0 + u^n) \cdot \mathbf{q} \, dx + \int_{\Omega} (|\lambda^n|^2 - 1)^{+2} (\mathbf{p}^0 + \lambda^n) \cdot \mathbf{q} \, dx \\ &+ 4 \int_{\Omega} (|\lambda^n|^2 - 1)^+ (\lambda^n \cdot \mathbf{p}^0) (\lambda^n \cdot \mathbf{q}) \, dx, \quad \forall \mathbf{q} \in \mathbf{Q}. \end{aligned} \quad (115)$$

Set

$$\mathbf{w}^0 = \mathbf{g}^0. \quad (116)$$

For $m \geq 0$, assuming that \mathbf{p}^m , \mathbf{g}^m and \mathbf{w}^m are known, the last two different from $\mathbf{0}$, we proceed as follows to compute $\{\mathbf{p}, \psi\}$:

Step 1. Descent

Solve

$$\bar{\psi}^m \in H_0^1(\Omega), \quad \alpha \int_{\Omega} \bar{\psi}^m \varphi \, dx + \int_{\Omega} \mu \nabla \bar{\psi}^m \cdot \nabla \varphi \, dx = -g \int_{\Omega} \mathbf{w}^m \cdot \nabla \varphi \, dx, \quad \forall \varphi \in H_0^1(\Omega), \quad (117)$$

and then

$$\begin{aligned} \bar{\mathbf{g}}^m \in \mathbf{Q}, \quad \int_{\Omega} \bar{\mathbf{g}}^m \cdot \mathbf{q} \, dx &= -\varepsilon \int_{\Omega} \nabla \bar{\psi}^m \cdot \mathbf{q} \, dx + \int_{\Omega} (|\lambda^n|^2 - 1)^{+2} \mathbf{w}^m \cdot \mathbf{q} \, dx + 4 \int_{\Omega} (|\lambda^n|^2 - 1)^+ (\lambda^n \cdot \mathbf{w}^m) (\lambda^n \cdot \mathbf{q}) \, dx, \\ \forall \mathbf{q} \in \mathbf{Q}. \end{aligned} \quad (118)$$

Compute

$$\rho_m = \frac{\int_{\Omega} |\bar{\mathbf{g}}^m|^2 \, dx}{\int_{\Omega} \bar{\mathbf{g}}^m \cdot \mathbf{w}^m \, dx} \quad (119)$$

and

$$\mathbf{p}^{m+1} = \mathbf{p}^m - \rho_m \mathbf{w}^m, \quad \mathbf{g}^{m+1} = \mathbf{g}^m - \rho_m \bar{\mathbf{g}}^m. \quad (120)$$

Step 2. Testing the convergence and construction of \mathbf{w}^{m+1}

If $\int_{\Omega} |\mathbf{g}^{m+1}|^2 dx / \int_{\Omega} |\mathbf{g}^0|^2 \leq \text{tol}_2$ take $\mathbf{p} = \mathbf{p}^{m+1}$ and compute ψ from the solution of

$$\alpha\psi - \mu \nabla^2 \psi = g \nabla \cdot \mathbf{p} \text{ in } \Omega, \quad \psi = 0 \text{ on } \Gamma;$$

else compute

$$\gamma_m = \frac{\int_{\Omega} |\mathbf{g}^{m+1}|^2 dx}{\int_{\Omega} |\mathbf{g}^m|^2 dx}, \quad (121)$$

and

$$\mathbf{w}^{m+1} = \mathbf{g}^{m+1} + \gamma_m \mathbf{w}^m. \quad (122)$$

Do $m = m + 1$ and return to (117).

Algorithm (113)–(122) is less complicated than it looks like; it requires essentially the solution of one Dirichlet problem at each iteration.

Remark 11. Algorithm (113)–(122) has been written in variational form in order to facilitate its finite element implementation, an issue to be addressed in Section 9.

8. Bingham flow in cylinders. (VI) An augmented Lagrangian approach to the solution of problem (58)

Problem (58) is equivalent to the following minimization one

$$u \in H_0^1(\Omega), \quad J(u) \leq J(v), \quad \forall v \in H_0^1(\Omega), \quad (123)$$

with

$$J(v) = \frac{1}{2} \int_{\Omega} [\alpha|v|^2 + \mu|\nabla v|^2] dx + g \int_{\Omega} |\nabla v| dx - \int_{\Omega} fv dx.$$

The idea behind the augmented Lagrangian method which follows is to uncouple nonlinearity and derivatives; this will be done by treating ∇v as an independent variable \mathbf{q} and then to impose the relation $\nabla v - \mathbf{q} = \mathbf{0}$ by penalization and the use of a Lagrange multiplier. In order to implement the above idea, we will proceed as follows:

(1) We denote $(L^2(\Omega))^2$ by \mathbf{Q} and define \mathbf{W} and $j(\cdot, \cdot)$ by

$$\mathbf{W} = \{ \{v, \mathbf{q}\} \mid v \in H_0^1(\Omega), \quad \mathbf{q} \in \mathbf{Q} \text{ and } \mathbf{q} = \nabla v \} \quad (124)$$

and

$$j(v, \mathbf{q}) = \frac{1}{2} \int_{\Omega} [\alpha|v|^2 + \mu|\nabla v|^2] dx + g \int_{\Omega} |\mathbf{q}| dx - \int_{\Omega} fv dx. \quad (125)$$

(2) We observe that problem (123) is equivalent to

$$\{u, \mathbf{p}\} \in \mathbf{W}, \quad j(u, \mathbf{p}) \leq j(v, \mathbf{q}), \quad \forall \{v, \mathbf{q}\} \in \mathbf{W}. \quad (126)$$

(3) We define an augmented Lagrangian functional $\mathcal{L}_r : (H_0^1(\Omega) \times \mathbf{Q}) \times \mathbf{Q} \rightarrow \mathbb{R}$ by

$$\mathcal{L}_r(\{v, \mathbf{q}\}, \boldsymbol{\mu}) = j(v, \mathbf{q}) + \frac{r}{2} \int_{\Omega} |\nabla v - \mathbf{q}|^2 dx + \int_{\Omega} \boldsymbol{\mu} \cdot (\nabla v - \mathbf{q}) dx \quad (127)$$

(with $r > 0$) and observe that if $\{\{u, \mathbf{p}\}, \boldsymbol{\lambda}\}$ is a saddle-point of \mathcal{L}_r over $(H_0^1(\Omega) \times \mathbf{Q}) \times \mathbf{Q}$, i.e., verifies

$$\begin{aligned} \{ \{u, \mathbf{p}\}, \boldsymbol{\lambda} \} &\in (H_0^1(\Omega) \times \mathbf{Q}) \times \mathbf{Q}, & \mathcal{L}_r(\{u, \mathbf{p}\}, \boldsymbol{\mu}) &\leq \mathcal{L}_r(\{u, \mathbf{p}\}, \boldsymbol{\lambda}) \leq \mathcal{L}_r(\{v, \mathbf{q}\}, \boldsymbol{\lambda}), \\ \forall \{ \{v, \mathbf{q}\}, \boldsymbol{\mu} \} &\in (H_0^1(\Omega) \times \mathbf{Q}) \times \mathbf{Q}, \end{aligned} \quad (128)$$

then, the pair $\{u, \mathbf{p}\}$ is the solution of problem (126), which implies in turn that u is the solution of problem (123) and that $\mathbf{p} = \nabla u$ (augmented Lagrangians, other than the one given by (127), can be used); we can in particular replace $\mu|\nabla v|^2$ in (125) by $\mu|\mathbf{q}|^2$, but it does not seem to make a significant difference from an algorithmic point of view.

(4) In order to solve the saddle-point problem (128), we advocate (following, e.g., Refs. [5,10,11,25,26]) the following Uzawa-type algorithm (called ALG2 in the above references):

$$u^{-1} \text{ and } \lambda^0 \text{ are given in } H_0^1(\Omega) \text{ and } \mathbf{Q}; \tag{129}$$

for $n \geq 0$, u^{n-1} and λ^n being known, solve

$$\mathbf{p}^n \in \mathbf{Q}, \quad \mathcal{L}_r(\{\mathbf{u}^{n-1}, \mathbf{p}^n\}, \lambda^n) \leq \mathcal{L}_r(\{\mathbf{u}^{n-1}, \mathbf{q}\}, \lambda^n), \quad \forall \mathbf{q} \in \mathbf{Q}, \tag{130}$$

then

$$u^n \in H_0^1(\Omega), \quad \mathcal{L}_r(\{u^n, \mathbf{p}^n\}, \lambda^n) \leq \mathcal{L}_r(\{v^n, \mathbf{p}^n\}, \lambda^n), \quad \forall v \in H_0^1(\Omega), \tag{131}$$

and update λ^n by

$$\lambda^{n+1} = \lambda^n + r(\nabla u^n - \mathbf{p}^n). \tag{132}$$

It follows from, e.g., [5,10,11,25,26], that the following convergence result holds:

$$\forall \{u^{-1}, \lambda^0\} \in H_0^1(\Omega) \times \mathbf{Q}, \text{ one has } \lim_{n \rightarrow \infty} \{\mathbf{u}^n, \mathbf{p}^n\} = \{\mathbf{u}, \nabla \mathbf{u}\} \text{ in } \mathbf{H}_0^1(\Omega) \times \mathbf{Q}, \tag{133}$$

where, in (133), u is the solution of problems (58) and (123). Concerning the implementation of algorithm (129)–(132), a close inspection shows that problem (130) reduces to:

$$\mathbf{p}^n = \text{Arg} \min_{\mathbf{q} \in \mathbf{Q}} \left[\frac{r}{2} \int_{\Omega} |\mathbf{q}|^2 dx + g \int_{\Omega} |\mathbf{q}| dx - \int_{\Omega} (r \nabla u^{n-1} + \lambda^n) \cdot \mathbf{q} dx \right]. \tag{134}$$

The minimization problem in (134) can be solved point-wise, leading to the following closed form solution for \mathbf{p}^n :

$$\text{a.e. on } \Omega, \mathbf{p}^n(\mathbf{x}) = \begin{cases} \frac{1}{r} \left(1 - \frac{g}{|\mathbf{X}^n(\mathbf{x})|} \right) \mathbf{X}^n(\mathbf{x}) & \text{if } |\mathbf{X}^n(\mathbf{x})| > g, \\ \mathbf{0} & \text{if } |\mathbf{X}^n(\mathbf{x})| \leq g, \end{cases} \tag{135}$$

with $\mathbf{X}^n = r \nabla u^{n-1} + \lambda^n$. On the other hand, (131) reduces to the following linear Dirichlet problem (written here in variational form):

$$u^n \in H_0^1(\Omega), \quad \alpha \int_{\Omega} u^n v dx + (\mu + r) \int_{\Omega} \nabla u^n \cdot \nabla v dx = \int_{\Omega} f v dx + \int_{\Omega} (r \mathbf{p}^n - \lambda^n) \cdot \nabla v dx, \quad \forall v \in H_0^1(\Omega); \tag{136}$$

the numerical solution of problems such as (136) is routine nowadays.

Remark 12. By updating λ^n after step (130) we obtain the following variant of algorithm (129)–(132):

$$u^{-1} \text{ and } \lambda^0 \text{ are given in } H_0^1(\Omega) \text{ and } \mathbf{Q}; \tag{137}$$

for $n \geq 0$, u^{n-1} and λ^n being known, solve

$$\mathbf{p}^n \in \mathbf{Q}, \quad \mathcal{L}_r(\{u^{n-1}, \mathbf{p}^n\}, \lambda^n) \leq \mathcal{L}_r(\{u^{n-1}, \mathbf{q}\}, \lambda^n), \quad \forall \mathbf{q} \in \mathbf{Q}, \tag{138}$$

update λ^n by

$$\lambda^{n+1/2} = \lambda^n + r(\nabla u^{n-1} - \mathbf{p}^n), \tag{139}$$

solve

$$u^n \in H_0^1(\Omega), \quad \mathcal{L}_r(\{u^n, \mathbf{p}^n\}, \lambda^{n+1/2}) \leq \mathcal{L}_r(\{v^n, \mathbf{p}^n\}, \lambda^{n+1/2}), \quad \forall v \in H_0^1(\Omega), \tag{140}$$

update $\lambda^{n+1/2}$ by

$$\lambda^{n+1} = \lambda^{n+1/2} + r(\nabla u^n - \mathbf{p}^n), \tag{141}$$

The above algorithm (called ALG3 in Refs. [5,10,11,25,26]) verifies also the convergence properties given in (133). The choice of r is for both algorithms a critical issue for which we refer to, e.g., Refs. [5,25]. Actually, both algorithms have very close relation with operator-splitting schemes such as Peaceman–Rachfords and Douglas–Rachfords (see the two above references for details). Concerning the relative merits of ALG2 and ALG3, let us say that it seems (see e.g. Refs. [5,25,26]) that ALG3 is faster for smooth problems while ALG2 is more robust; since the problem under consideration involves the non-differentiable function $v \rightarrow \int_{\Omega} |\nabla v| dx$, we favored ALG2.

9. Bingham flow in cylinders. (VII) Finite element approximation

In Section 6, Remark 6, we have been advocating the use of low order space-time approximations for Bingham flow in cylinders, the main reason being the relative low regularity of the solutions. From these considerations, the backward Euler scheme (discussed in Section 6) will be our method of choice for the time-discretization. Similarly, we will rely on globally continuous, piecewise affine finite approximations for the space discretization. This combination leads us to the schemes (43) and (44) described in Section 6, Remark 6. We have thus to solve at each time step a finite dimensional problem of the following type:

$$u_h \in V_{0h}, \quad \alpha \int_{\Omega_h} u_h(v - u_h) dx + \mu \int_{\Omega_h} \nabla u_h \cdot \nabla(v - u_h) dx + g[j_h(v) - j_h(u_h)] \geq \int_{\Omega_h} f_h(v - u_h) dx, \quad \forall v \in V_{0h}, \quad (142)$$

with

$$j_h(v) = \int_{\Omega_h} |\nabla v| dx = \sum_{K \in \mathcal{T}_h} \int_K |\nabla v| dx. \quad (143)$$

The finite dimensional problem (142) has a unique solution characterized by the existence of λ_h such that

$$\{u_h, \lambda_h\} \in V_{0h} \times \Lambda_h, \quad \alpha \int_{\Omega_h} u_h v dx + \mu \int_{\Omega_h} \nabla u_h \cdot \nabla v dx + g \int_{\Omega_h} \lambda_h \cdot \nabla v dx = \int_{\Omega_h} f_h v dx, \quad \forall v \in V_{0h},$$

$$\lambda_h \cdot \nabla u_h = |\nabla u_h|, \quad (144)$$

with

$$\Lambda_h = \{\mu \mid \mu \in L^2(\Omega_h) \times L^2(\Omega_h), \quad \forall K \in \mathcal{T}_h, \quad \mu|_K = \mu_K \in \mathbb{R}^2, \quad |\mu_K| \leq 1\}. \quad (145)$$

System (144) takes various equivalent forms, among them

$$u_h \in V_{0h}, \quad \alpha \int_{\Omega_h} u_h v dx + \mu \int_{\Omega_h} \nabla u_h \cdot \nabla v dx + g \int_{\Omega_h} \lambda_h \cdot \nabla v dx = \int_{\Omega_h} f_h v dx, \quad \forall v \in V_{0h},$$

$$\lambda_h = P_{\Lambda_h}(\lambda_h + rg \nabla u_h), \quad \forall r \geq 0, \quad (146)$$

and

$$\{u_h, \lambda_h\} \in V_{0h} \times \Lambda_h, \quad \alpha \int_{\Omega_h} u_h v dx + \mu \int_{\Omega_h} \nabla u_h \cdot \nabla v dx + g \int_{\Omega_h} \lambda_h \cdot \nabla v dx = \int_{\Omega_h} f_h v dx, \quad \forall v \in V_{0h},$$

$$- \int_{\Omega_h} \nabla u_h \cdot (\mu - \lambda_h) dx \geq 0, \quad \forall \mu \in \Lambda_h; \quad (147)$$

above, P_{Λ_h} is the orthogonal projection operator from $\mathbf{L}_h (= \{\mu \mid \mu \in L^2(\Omega_h) \times L^2(\Omega_h), \forall K \in \mathcal{T}_h, \mu|_K = \mu_K \in \mathbb{R}^2\})$ onto Λ_h ; it verifies

$$P_{\Lambda_h}(\mu)|_K = \frac{\mu_K}{\max(1, |\mu_K|)}, \quad \forall K \in \mathcal{T}_h, \quad \forall \mu \in \mathbf{L}_h. \quad (148)$$

From these formulations, deriving the fully discrete analogues of the various iterative methods discussed in the preceding sections is straightforward.

10. Bingham flow in cylinders. (VIII) Numerical experiments

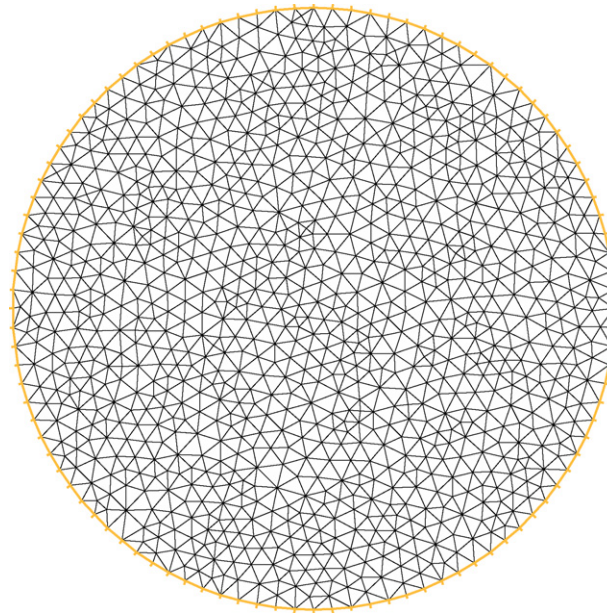
In this section, we will focus on the solution of the steady flow problem (52) in the particular case where Ω is the *disk* defined by

$$\Omega = \{x \mid x = \{x_1, x_2\}, \quad x_1^2 + x_2^2 < R^2\}. \quad (149)$$

Assume that $C \geq 0$, then for the above cross-section, the solution of (52) is given by

$$u_\infty(x) = \begin{cases} \left(\frac{R-r}{2\mu}\right) \left[\frac{C}{2}(R+r) - 2g\right] & \text{if } R' \leq r \leq R, \\ \left(\frac{R-R'}{2\mu}\right) \left[\frac{C}{2}(R+R') - 2g\right] & \text{if } 0 \leq r \leq R', \end{cases} \quad (150)$$

with $r = \sqrt{x_1^2 + x_2^2}$ and $R' = 2g/C$.

Fig. 1. A triangulation \mathcal{T}_h of the disk Ω .

For the numerical experiments described below, we took $R = 1/4$, $C = 16$, and $\mu = 1/4$, implying that $u_\infty = 0$ if $g \geq 2$. To approximate the related problem (52) we have used the finite element spaces described in Section 9, defined from triangulations of Ω like the one shown in Fig. 1, below (with h the length of the largest edge(s) of the triangulation).

In Table 1, we have reported, for various values of g and h , some of the numerical results obtained by applying, to the solution of problem (52), the discrete variant of algorithm (61)–(63) (with $\alpha = 0$ and $f = C$), associated to the triangulation \mathcal{T}_h . The above algorithm has been initialized with $\lambda_h^0 = \mathbf{0}$ and we stopped iterating as soon as $\|\lambda_h^{n+1} - \lambda_h^n\|_{L^2} \leq 10^{-4}$, *nit* being the corresponding number of iterations; for r we took μ/g^2 . For $h = 1/64$ (resp., $1/128$ and $1/256$), \mathcal{T}_h consists of 1976 (resp., 7,945 and 31,690) triangles and has 1,039 (resp., 4074 and 16,047) vertices. The results shown in Table 1 (and Fig. 2) suggest that $\|u_h - u\|_{L^2(\Omega)} \approx O(h^2)$, while $\|\nabla(u_h - u)\|_{(L^2(\Omega))^2} \approx O(h)$; these results are consistent with error estimates proved in, e.g., [10].

The results shown in Table 2 concern the same test problem and have been obtained using the same triangulations than above. On the other hand for these computations we have used the nested iterative method obtained by combining the (pseudo-) time discretization schemes (87) and (88) (initialized with $\lambda_h^0 = \mathbf{0}$) with algorithm (90)–(92) (initialized with $\lambda_{h,0}^n = \lambda_h^{n-1}$). We took $\Delta\tau = 2\mu/g^2$, $r = \Delta\tau/2$, and stop iterating as soon as $\|\lambda_h^n - \lambda_h^{n+1}\|_{L^2} \leq 10^{-4}$ (outer iterations) and $\|\lambda_{h,k+1}^n - \lambda_{h,k}^n\|_{L^2} \leq 10^{-5}$ (inner iterations) (other stopping strategies are possible). The numbers in the *nit* column correspond to outer iterations. We observe that the approximation errors given in Table 2 are of the same order as those in Table 1.

Table 1
Numerical results obtained by the discrete variant of algorithm (61)–(63)

g	h	<i>nit</i>	$\ u_h - u\ _{L^2}$	$\ \nabla(u_h - u)\ _{L^2}$
0.2	1/64	4	1.2206E – 004	1.0964E – 002
	1/128	4	3.0895E – 005	4.9999E – 003
	1/256	3	7.6938E – 006	2.7501E – 003
1.0	1/64	15	1.0071E – 004	2.1055E – 002
	1/128	8	2.4395E – 005	1.0090E – 002
	1/256	5	6.1040E – 006	5.1368E – 003
1.7	1/64	20	1.3162E – 004	1.8784E – 002
	1/128	7	2.8520E – 005	8.0858E – 003
	1/256	2	5.3213E – 006	4.0120E – 003
1.9	1/64	2	6.3682E – 005	1.1223E – 002
	1/128	2	1.5250E – 005	4.8720E – 003
	1/256	2	4.5102E – 006	2.4759E – 003
2.1	1/64	2	5.1227E – 015	5.2260E – 014
	1/128	2	3.2679E – 014	3.1831E – 013
	1/256	2	2.0857E – 013	2.0147E – 012

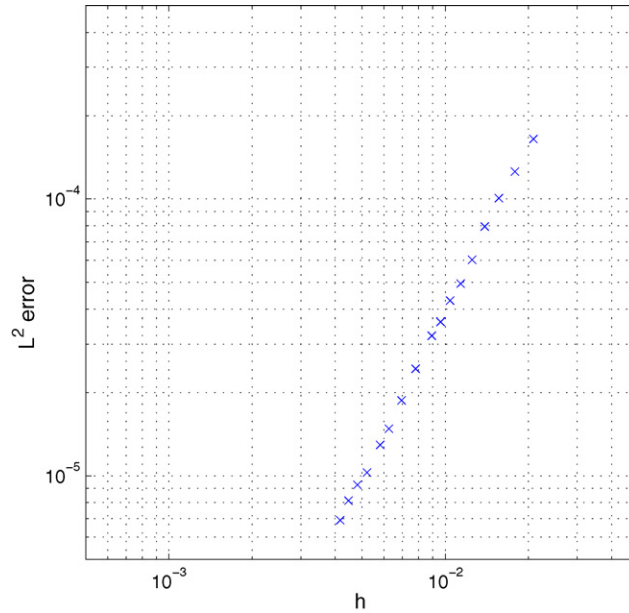


Fig. 2. Variation of $\|u - u_h\|_{L^2(\Omega)}$ vs. h for $g = 1$ (log scales).

Table 2

Numerical results obtained by the discrete variant of algorithm (87), (88), (90)–(92)

g	h	nit	$\ u_h - u\ _{L^2}$	$\ \nabla(u_h - u)\ _{L^2}$
0.2	1/64	3	1.2213E - 004	1.0959E - 002
	1/128	3	3.0872E - 005	4.9971E - 003
	1/256	3	7.6864E - 006	2.7502E - 003
1.0	1/64	14	1.0055E - 004	2.1043E - 002
	1/128	7	2.3587E - 005	1.0061E - 002
	1/256	5	5.8432E - 006	5.1390E - 003
1.7	1/64	20	1.2672E - 004	1.8807E - 002
	1/128	7	1.9826E - 005	8.1015E - 003
	1/256	6	4.8495E - 006	4.1762E - 003
1.9	1/64	7	1.0990E - 004	1.1936E - 002
	1/128	7	1.7497E - 005	5.3066E - 003
	1/256	7	4.6899E - 006	2.6584E - 003
2.1	1/64	7	3.3682E - 017	3.8609E - 016
	1/128	7	2.1175E - 016	2.0748E - 015
	1/256	7	2.3071E - 015	2.2257E - 014

Finally, we have shown in Table 3 (and Figs. 3 and 4) the results obtained using a discrete variant of the Penalty/Newton/Uzawa/conjugate gradient method discussed in Section 7.5. The computations have been done taking $h = 1/128$ and varying g and the penalty parameter ε . The Newton's (resp., Uzawa/conjugate gradient) iterations have been initialized with $\lambda_h^0 = \mathbf{0}$ (resp., $\mathbf{p}_h^0 = \mathbf{0}$) and (using Section 7.5 notation) we took $\text{tol}_1 = 10^{-6}$ and $\text{tol}_2 = 10^{-4}$ in the stopping criteria. In Table 3, *nit* is the number of Newton's iterations necessary to achieve convergence. We observe that the number of Newton's iterations decreases with g ; this property was expected since the size of the fluid region (where $|\lambda(x)| = 1$) is a decreasing function of g , everything else being the same; on the other hand, the number of Uzawa/conjugate gradient iterations stays around 5, for the values of g and ε considered here. Fig. 3, which corresponds to $g = 1$, suggest that for ε moderately small $\|u_{h,\varepsilon} - u_h^*\|_{L^2(\Omega)}$ varies like $\sqrt{\varepsilon}$ (which is what was expected), while it stays constant for smaller values of ε . We suspect that to recover the $\sqrt{\varepsilon}$ behavior, for the very small values of ε , we should use smaller tolerances in the stopping criteria of the various iterative methods used to compute $u_{h,\varepsilon}$ and u_h^* (u_h^* is the approximate solution computed via algorithm (61)–(63)). In Fig. 4, we compare, for $g = 1$, the exact solution with the approximated ones, obtained with $h = 1/128$ and various values of ε ; we observe that the condition $\nabla u = \mathbf{0}$ is well approximated in the rigidity region.

We will conclude this discussion, concerning the numerical simulation of Bingham flow in cylinders by mentioning that, if one is interested by the steady state solution only, it may be advantageous to consider the following (non-physical) initial

Table 3

Numerical results obtained by the penalty/Newton/ Uzawa/conjugate gradient method of Section 7.5 for $h = 128$ (u_h^* is the corresponding solution obtained by the related discrete variant of algorithm (61)–(63))

g	ε	nit	$\ u_{h,\varepsilon} - u_h^*\ _{L^2}$	$\ u_{h,\varepsilon} - u\ _{L^2}$	$\ \nabla(u_{h,\varepsilon} - u)\ _{L^2}$
0.2	1E-003	19	5.4330E - 004	5.4523E - 004	7.2570E - 003
	1E-005	19	6.7749E - 005	7.5271E - 005	5.0353E - 003
	1E-007	19	4.5020E - 005	5.5144E - 005	5.0137E - 003
1.0	1E-003	11	3.2531E - 003	3.2621E - 003	3.6440E - 002
	1E-005	11	3.9400E - 004	4.0331E - 004	1.0732E - 002
	1E-007	11	2.4255E - 004	2.5211E - 004	1.0257E - 002
1.7	1E-003	9	1.3728E - 003	1.3978E - 003	2.6178E - 002
	1E-005	6	3.8398E - 004	4.0890E - 004	1.0300E - 002
	1E-007	6	3.6026E - 004	3.8519E - 004	1.0092E - 002
1.9	1E-003	11	3.8816E - 004	4.0174E - 004	1.4630E - 002
	1E-005	4	1.4912E - 004	1.6300E - 004	6.4455E - 003
	1E-007	4	1.4636E - 004	1.6024E - 004	6.4008E - 003
2.1	1E-003	2	3.2679E - 014	2.6906E - 028	2.7906E - 027
	1E-005	2	3.2679E - 014	2.6728E - 028	2.7729E - 027
	1E-007	2	3.2679E - 014	2.6958E - 028	2.7919E - 027

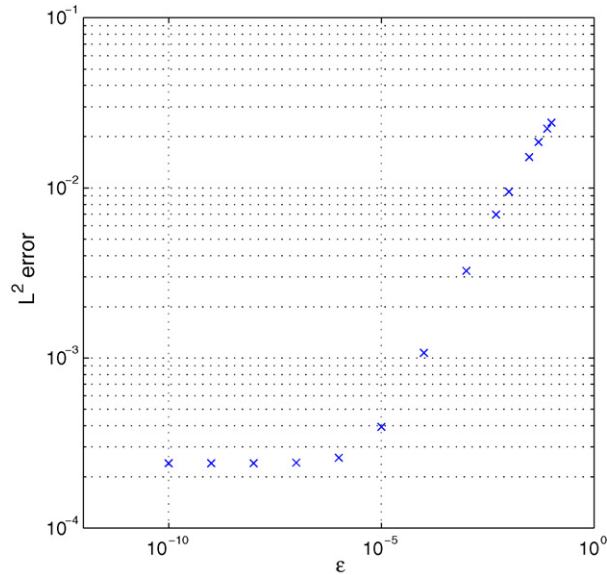


Fig. 3. Variation of $\|u_{h,\varepsilon} - u_h^*\|_{L^2(\Omega)}$ vs. ε for $h = 1/128$ and $g = 1$.

value problem:

$$\begin{aligned}
 u(0) &= u_0 (\in H_0^1(\Omega)), \quad \int_{\Omega} \nabla(\partial_t u) \cdot \nabla(v - u) \, dx + \mu \int_{\Omega} \nabla u \cdot \nabla(v - u) \, dx + g \left[\int_{\Omega} |\nabla v| \, dx - \int_{\Omega} |\nabla u| \, dx \right] \\
 &\geq C \int_{\Omega} (v - u) \, dx, \quad \forall v \in H_0^1(\Omega),
 \end{aligned}
 \tag{151}$$

where $dC/dt = 0$. Indeed, suppose that u_{∞} is the solution of the corresponding steady state problem (52); it is then fairly easy to prove that

$$\|u(t) - u_{\infty}\|_{H_0^1(\Omega)} \leq \|u(t) - u_{\infty}\|_{H_0^1(\Omega)} \exp^{-\mu t}, \quad \forall t \geq 0,
 \tag{152}$$

a stronger convergence result than the one given by (23) in Section 5. We refer to [12] concerning the practical implementation of the above approach (which is no more complicated to implement than the one based on (17)).

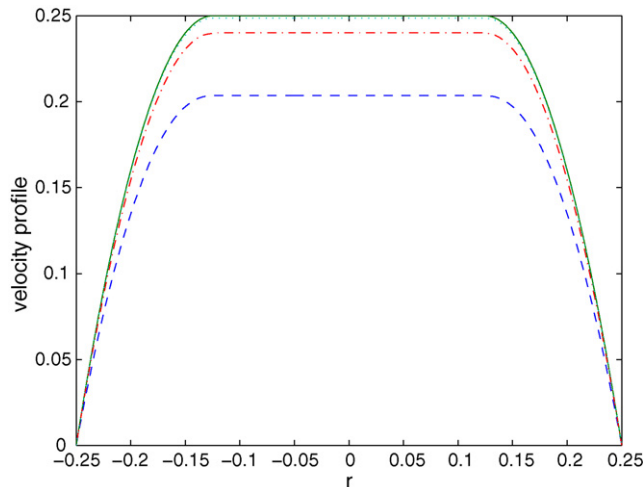


Fig. 4. Graphs of the exact solution (—) and of the approximated solutions restricted to a diameter of Ω for $\varepsilon = 3 \times 10^{-2}$ (---), 10^{-3} (-·-·-) and 10^{-5} (···) ($h = 1/128$ and $g = 1$).

11. Bingham flow in cavities

11.1. Generalities

The modeling of multidimensional Bingham flow can be found in Section 2. From now on, we will assume that Ω is a bounded region of \mathbb{R}^d (with $d = 2$ or 3). The numerical simulation of such flow has been addressed in, e.g., ([7], Chapter 10), [27,28] (see also the references therein). In this article, we will briefly review the operator-splitting based methodology discussed in the three above references and present some numerical results obtained with it. Before describing the above methodology, let us mention that a popular approach to overcome the difficulties associated with the non-differentiability of the functional $\mathbf{v} \rightarrow \int_{\Omega} |\mathbf{D}(\mathbf{v})| \, dx$ is to approximate the problems (1)–(5) and (6)–(9) by regularization; among the various possible regularization procedures, the one below is classical

$$\varrho[\partial_t \mathbf{u}_\varepsilon + (\mathbf{u}_\varepsilon \cdot \nabla) \mathbf{u}_\varepsilon] = \nabla \cdot \boldsymbol{\sigma}_\varepsilon + \mathbf{f} \quad \text{in } \Omega \times (0, T), \quad (153)$$

$$\nabla \cdot \mathbf{u}_\varepsilon = 0 \quad \text{in } \Omega \times (0, T), \quad (154)$$

$$\boldsymbol{\sigma}_\varepsilon = -p_\varepsilon \mathbf{I} + \frac{\sqrt{2}g \mathbf{D}(\mathbf{u}_\varepsilon)}{(\varepsilon^2 + |\mathbf{D}(\mathbf{u}_\varepsilon)|^2)^{1/2}} + 2\mu \mathbf{D}(\mathbf{u}_\varepsilon), \quad (155)$$

$$\mathbf{u}_\varepsilon(0) = \mathbf{u}_0, \quad (156)$$

$$\mathbf{u}_\varepsilon = \mathbf{u}_B \quad \text{on } \Gamma \times (0, T). \quad (157)$$

The main drawback of the above regularization procedure is that it does not have the property that $\mathbf{u}(t)$ reaches the value $\mathbf{0}$ in finite time if $\mathbf{f} = \mathbf{0}$ (unlike the solutions of (1)–(5) and (6)–(9)). We will not investigate furthermore the regularization approach associated with (153)–(157). Instead, in the following sections, we will discuss the solution of problem (6)–(9) via a *time-discretization by operator-splitting*; with this approach (already investigated in Refs. ([7], Chapter 10), [27,28]) we will be able to solve problem (6)–(9) via a methodology closely related to various methods used for the solution of the Navier–Stokes equations modeling incompressible Newtonian viscous flow (i.e., those equations obtained by taking $g = 0$ in (1)–(5) and (6)–(9)).

11.2. Time-discretization of problem (6)–(9) by operator splitting

There are many ways to discretize problem (6)–(9) by operator splitting. Among the many possible schemes, we will discuss only one, of the Marchuk–Yanenko type (see ([7], Chapter 6) and the references therein); this scheme reads as follows (with, as usual, $t^{n+\alpha} = (n + \alpha)\Delta t$):

$$\mathbf{u}^0 = \mathbf{u}_0; \quad (158)$$

then, for $n \geq 0$, \mathbf{u}^n being known, we compute $\{\mathbf{u}^{n+1/3}, p^{n+1}\}$, $\mathbf{u}^{n+2/3}$ and \mathbf{u}^{n+1} as follows:

Solve the generalized Stokes problem

$$\begin{aligned} \frac{\varrho}{\Delta t}(\mathbf{u}^{n+1/3} - \mathbf{u}^n) - \frac{\mu}{2}\nabla^2\mathbf{u}^{n+1/3} + \nabla p^{n+1} &= \mathbf{f}^{n+1}(= \mathbf{f}(t^{n+1})) \text{ in } \Omega, & \nabla \cdot \mathbf{u}^{n+1/3} &= 0 \text{ in } \Omega, \\ \mathbf{u}^{n+1/3} &= \mathbf{u}_B^{n+1}(= \mathbf{u}_B(t^{n+1})) \text{ on } \Gamma, \end{aligned} \tag{159}$$

then the transport problem

$$\partial_t \mathbf{u} + (\mathbf{u}^{n+1/3} \cdot \nabla)\mathbf{u} = 0 \text{ in } \Omega \times (t^n, t^{n+1}), \quad \mathbf{u}(t^n) = \mathbf{u}^{n+1/3}, \quad \mathbf{u} = \mathbf{u}_B^{n+1} \text{ on } \Gamma_-^{n+1} \times (t^n, t^{n+1}), \tag{160}$$

and set

$$\mathbf{u}^{n+2/3} = \mathbf{u}(t^{n+1}); \tag{161}$$

finally, solve the elliptic variational inequality problem

$$\begin{aligned} \mathbf{u}^{n+1} \in (H^1(\Omega))^d, \quad \mathbf{u}^{n+1} = \mathbf{u}_B^{n+1} \text{ on } \Gamma, \quad \varrho \int_{\Omega} (\mathbf{u}^{n+1} - \mathbf{u}^{n+2/3}) \cdot (\mathbf{v} - \mathbf{u}^{n+1}) \, dx + \frac{\mu \Delta t}{2} \int_{\Omega} \nabla \mathbf{u}^{n+1} : \nabla (\mathbf{v} - \mathbf{u}^{n+1}) \, dx \\ + g\sqrt{2}\Delta t [j(\mathbf{v}) - j(\mathbf{u}^{n+1})] \geq 0, \quad \forall \mathbf{v} \in (H^1(\Omega))^d, \quad \mathbf{v} = \mathbf{u}_B^{n+1} \text{ on } \Gamma; \end{aligned} \tag{162}$$

in (160) we have $\Gamma_-^{n+1} = \{x|x \in \Gamma, (\mathbf{u}_B^{n+1} \cdot \mathbf{n})(x) < 0\}$, \mathbf{n} being the outward unit normal vector at Γ . Closely related operator splitting techniques have been used in [27] for the simulation of Bingham flow in two dimensional square cavities.

Remark 13. It follows from, e.g., ([10], Chapters 1 and 2) that the variational inequality problem (162) has a unique solution characterized by the existence of a $d \times d$ tensor-valued function λ^{n+1} such that

$$\begin{aligned} \frac{\varrho}{\Delta t}(\mathbf{u}^{n+1} - \mathbf{u}^{n+2/3}) - \frac{\mu}{2}\nabla^2\mathbf{u}^{n+1} - g\sqrt{2}\nabla \cdot \lambda^{n+1} &= \mathbf{0} \text{ in } \Omega, \quad \mathbf{u}^{n+1} = \mathbf{u}_B^{n+1} \text{ on } \Gamma, \quad \lambda^{n+1} \in (L^\infty(\Omega))^{d \times d}, \quad \lambda^{n+1} = (\lambda^{n+1})^t, \\ |\lambda^{n+1}(x)| &\leq 1 \text{ a.e. on } \Omega, \quad \lambda^{n+1}(x) : \mathbf{D}(\mathbf{u}^{n+1})(x) = |\mathbf{D}(\mathbf{u}^{n+1})(x)| \text{ a.e. on } \Omega. \end{aligned} \tag{163}$$

The multiplier λ^{n+1} is not necessarily unique.

11.3. On the computer implementation of scheme (158)–(162)

There is no room in this review article to give a detailed discussion of the computer implementation of scheme (158)–(162) (if one takes $g = 0$ in step (162) one recovers a solution method for the Navier–Stokes equations modeling incompressible Newtonian viscous flow); such a discussion can be found in ([7], Chapter 10) and [28]. In the present article, our discussion will be limited to the following comments:

- (1) After an appropriate space discretization, the generalized Stokes problem (159) can be solved efficiently by an Uzawa-conjugate gradient algorithm, preconditioned by discrete Poisson–Neumann solvers. A detailed discussion of these Stokes solvers (including an historical account) can be found in, e.g., ([7], Chapter 5).
- (2) To solve the transport problem (160), we have advocated in ([7], Chapter 10) and [28] its equivalence with the following wave-like equation problem (written directly in variational form):

Find \mathbf{u} such that

$$\begin{aligned} \int_{\Omega} \partial_t^2 \mathbf{u} \cdot \mathbf{v} \, dx + \int_{\Omega} (\mathbf{u}^{n+1/3} \cdot \nabla)\mathbf{u} \cdot (\mathbf{u}^{n+1/3} \cdot \nabla)\mathbf{v} \, dx + \int_{\Gamma \setminus \Gamma_-^{n+1}} (\mathbf{u}^{n+1/3} \cdot \mathbf{n})(\partial_t \mathbf{u} \cdot \mathbf{v}) \, d\Gamma = 0, \\ \forall \mathbf{v} \in V_{0,-}^{n+1}, \text{ a.e. on } (t^n, t^{n+1}), \quad \mathbf{u} = \mathbf{u}_B^{n+1} \text{ on } \Gamma_-^{n+1} \times (t^n, t^{n+1}), \quad \mathbf{u}(t^n) = \mathbf{u}^{n+1/3}, \quad \partial_t \mathbf{u}(t^n) = -(\mathbf{u}^{n+1/3} \cdot \nabla)\mathbf{u}^{n+1/3}, \end{aligned} \tag{164}$$

with the test function space $V_{0,-}^{n+1}$ defined by

$$V_{0,-}^{n+1} = \{\mathbf{v} \mid \mathbf{v} \in (H^1(\Omega))^d, \mathbf{v} = \mathbf{0} \text{ on } \Gamma_-^{n+1}\}.$$

The solution of problem (160), via its equivalent formulation (164), has been discussed at length in [7], where it has been validated by the results of numerical experiments for a large variety of two and three dimensional test problems. In particular, the space-time discretization of problem (164) by a combination of finite element space approximations and well-chosen finite difference time discretization schemes is relatively easy to implement and leads to non-dissipative and accurate methods (see, e.g., [7], and the references therein, for details).

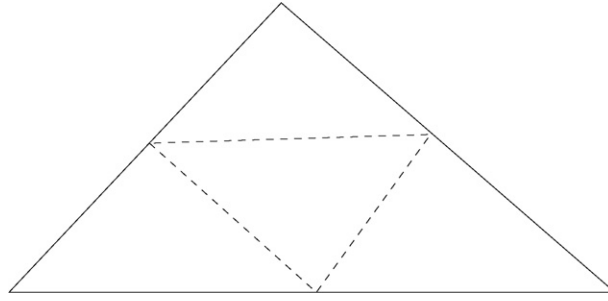


Fig. 5. Dividing K belonging to \mathcal{T}_h to define $\mathcal{T}_{h/2}$.

- (3) Problem (162) is a trivial vector-valued variant of problem (58) in Section 7.3, implying that the various methods we have considered for the solution of (58) are easy to modify in order to solve (162). Some of the methods resulting of these modifications are described in, e.g., ([7], Chapter 10) and [28].
- (4) Concerning the space discretization of problem (500)–(504), we have relied, in Refs. [7,28], on a variant of the well-known Bercovier–Pironneau finite element approximation. Assuming, for simplicity, that Ω is a polygonal domain of \mathbb{R}^2 , one uses the following finite element spaces to approximate pressure and velocity, respectively:

$$P_h = \{q \mid q \in C^0(\bar{\Omega}), \quad q|_K \in P_1, \quad \forall K \in \mathcal{T}_h\}, \quad \mathbf{V}_h = \{\mathbf{v} \mid \mathbf{v} \in (C^0(\bar{\Omega}))^2, \quad \mathbf{v}|_K \in (P_1)^2, \quad \forall K \in \mathcal{T}_{h/2}\},$$

where-as usual- P_1 is the space of the polynomials of two variables of degree ≤ 1 , and where $\mathcal{T}_{h/2}$ is the triangulation of Ω , obtained from the pressure triangulation \mathcal{T}_h by joining the mid-points of the edges of its elements (as shown in Fig. 5, below).

We observe that it is easy to compute $j(\mathbf{v})$, $\forall \mathbf{v} \in \mathbf{V}_h$, since (from the definition of \mathbf{V}_h) we have $\mathbf{D}(\mathbf{v}|_K) \in (P_0)^{2 \times 2}$, $\forall K \in \mathcal{T}_{h/2}$, and therefore $|\mathbf{D}(\mathbf{v}|_K)| \in P_0$ (with P_0 the space of the constant functions of two variables), which implies in turn that

$$j(\mathbf{v}) = \int_{\Omega} |\mathbf{D}(\mathbf{v})| \, dx = \sum_{K \in \mathcal{T}_{h/2}} \text{meas.}(K) |\mathbf{D}(\mathbf{v}|_K)|, \quad \forall \mathbf{v} \in \mathbf{V}_h.$$

There is no need thus for numerical integration to compute $j(\mathbf{v})$. The finite element approximation of the sub-problems (159) (160) and (162), and the solution of the resulting fully discrete problems is discussed in Refs. [7,28].

11.4. Numerical experiments and further comments

The computational methodology (briefly) discussed in Section 11.3 has been applied to the solution of problem (6)–(9), assuming that:

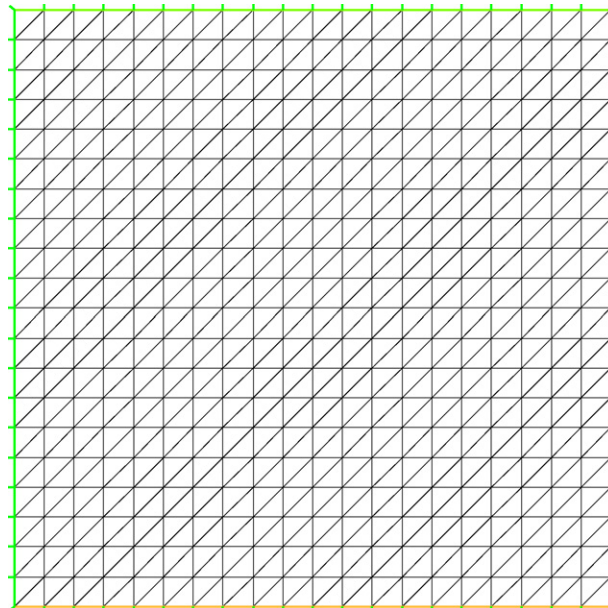


Fig. 6. A uniform triangulation of Ω .

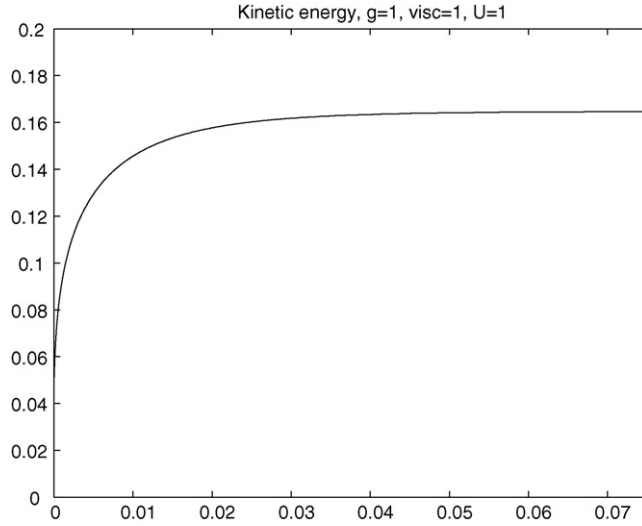


Fig. 7. Variation of the kinetic energy.

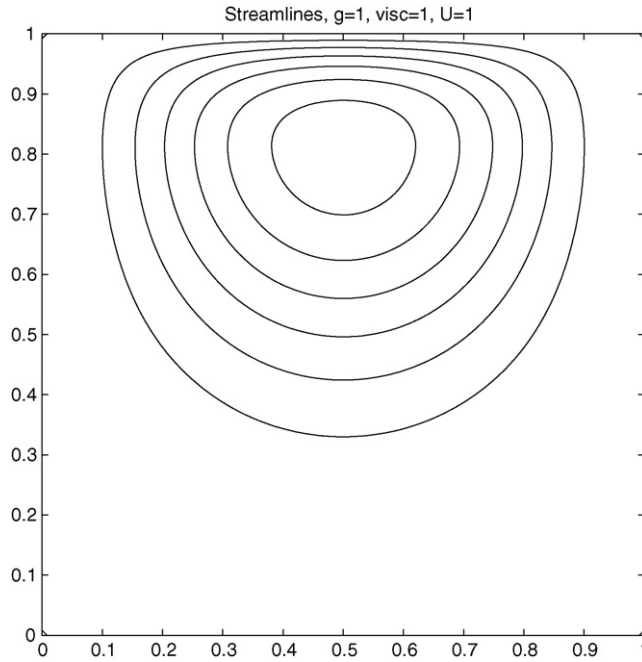


Fig. 8. Streamlines of the computed velocity field at steady state.

- (1) $\Omega = (0, 1) \times (0, 1)$, $\Gamma = \partial\Omega$.
- (2) $\varrho = 1$, $\mu = 1$, $g = 1$.
- (3) $\Gamma_N = \{x \mid x = \{x_1, x_2\}, x_2 = 1, 0 < x_1 < 1\}$ and (sliding upper boundary)

$$\mathbf{u}_B(x) = \begin{cases} \mathbf{0} & \text{if } x \in \Gamma \setminus \Gamma_N, \\ 16\{x_1^2(1-x_1)^2, 0\} & \text{if } x \in \Gamma_N \end{cases} \quad (165)$$

- (4) $\mathbf{u}_0 = \mathbf{0}$.

Remark 14. The methodology discussed in Sections 11.2 and 11.3 is robust enough to handle without additional difficulties the case where \mathbf{u}_B given by (165) would be replaced by

$$\mathbf{u}_B(x) = \begin{cases} \mathbf{0} & \text{if } x \in \Gamma \setminus \Gamma_N, \\ \{1, 0\} & \text{if } x \in \Gamma_N. \end{cases} \quad (166)$$

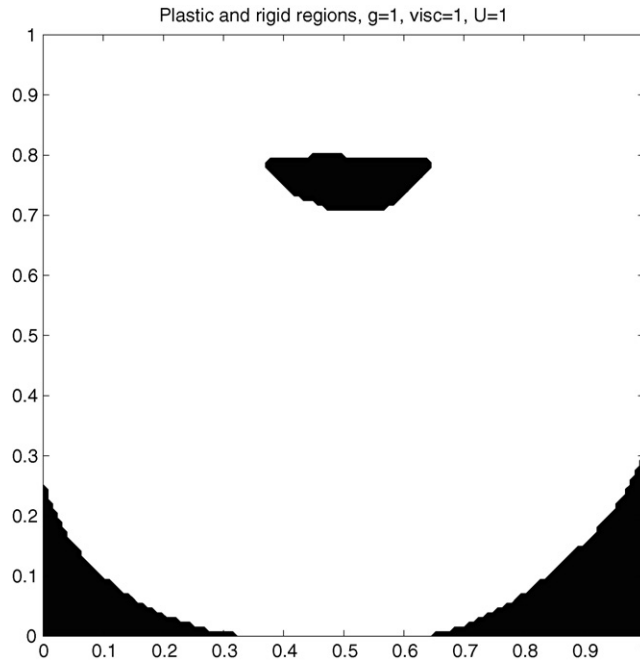


Fig. 9. Visualization of the computed plastic (white) and rigid (black) regions at steady state.

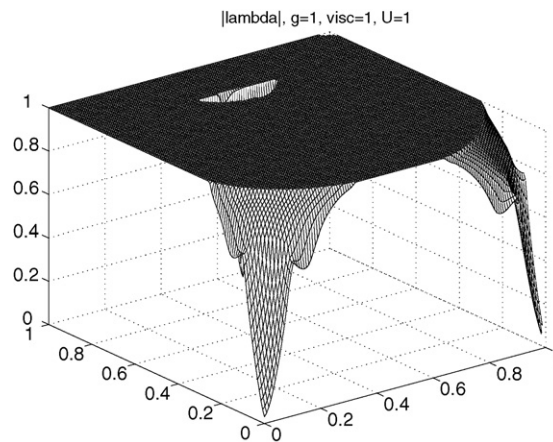


Fig. 10. Graph of $|\lambda_h|$ (λ_h is the computed approximation of λ).

The regularization associated to (165) is a classical one in the context of wall driven cavity flow, which is the main reason why we used it here.

The results shown below have been obtained using for \mathcal{T}_h a uniform triangulation like the one shown in Fig. 6, below, but with a smaller space discretization step, namely $\Delta x_1 = \Delta x_2 = 1/64$; for the time discretization, we took $\Delta t = 10^{-3}$.

On Fig. 7, we have visualized the time variation of the computed kinetic energy; it is clear from this figure that we have fast convergence to a steady flow. On Fig. 8 we have shown the streamlines of the (quasi) steady-state solution. The rigidity (black) and plastic (white) regions have been visualized on Fig. 9. The rigidity region is the one where $\mathbf{D}(\mathbf{u}) = \mathbf{0}$; it reconnects tangentially with the boundary of Ω in the two lower corners, as shown in the above figure, and in Fig. 10 where the graph of the function $x \rightarrow |\lambda(x)|$ has been visualized (we recall that $|\lambda(x)| = 1$ in the plastic region). The above results are in good agreement with those reported in [27].

To conclude the presentation of the results associated to the test problem under consideration, we will report on the following numerical experiment: with \mathbf{u}_0 , μ , g and \mathbf{u}_B as above, we solved – approximately – problems (6)–(9) up to $t = 0.05$; let us denote by $\mathbf{u}_h(0.05)$ the approximate velocity at $t = 0.05$. At $t = 0.05$, we froze the motion of the upper wall implying that for $t > 0.05$ the Bingham flow is still modeled by (6)–(9) completed by the boundary condition

$$\mathbf{u}(t) = \mathbf{0} \quad \text{on } \Gamma, \quad \text{if } t \geq 0.05,$$

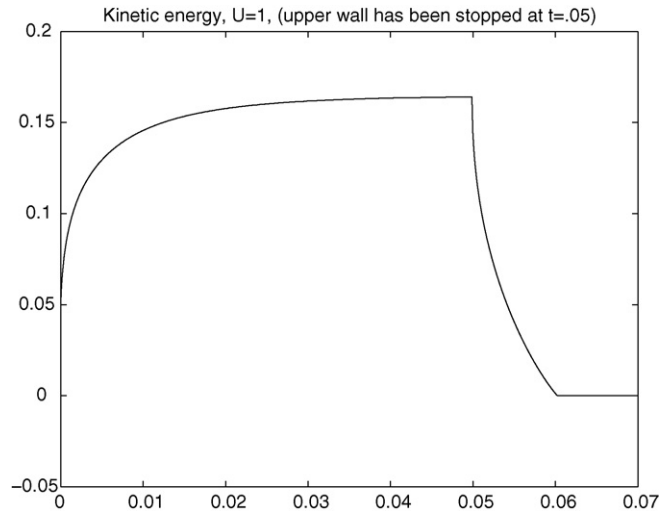


Fig. 11. Variation of the kinetic energy vs. time after the sliding of the upper wall has been stopped at $t = 0.05$.

with $\mathbf{u}_h(0.05)$ as initial condition at $t = 0.05$. Fig. 11 suggests that the flow behaves as expected, namely, the fluid returns to rest in finite time. The kinetic energy behavior observed in the above figure is consistent with the one reported in [5,11,30], concerning the solution of a closely related test problem (in the three above references the solution was computed using an equivalent stream-function formulation of problem(6)–(9), coupled to a variant of the augmented Lagrangian algorithm (128)–(131)).

12. Conclusions

Various computational methods for the numerical simulation of Bingham visco-plastic flow have been discussed in the preceding sections of this article. Since some of them still have to be tested for multi-dimensional flow in general geometry, the authors do not think they have enough practical experience to give strong advices on which method has to be used. Actually picking a method among others largely depends on the existing software the potential user has access to. At that stage let us say that the Penalty/Newton/Conjugate Gradient method discussed in Section 7.5 looks promising to us and we intend to apply it in the near future to the solution of problems more complicated than flow in cylinders.

Acknowledgment

The support by NSF (Grant DMS-0209066) is acknowledged.

References

- [1] G. Duvaut, J.L. Lions, *Les Inéquations en Mécanique et en Physique*, Dunod, Paris, 1972.
- [2] G. Duvaut, J.L. Lions, *Inequalities in Mechanics and Physics*, Springer, Berlin, 1976.
- [3] W. Prager, *Introduction to Mechanics of Continua*, Ginn and Company, Boston, MA, 1961.
- [4] P. Germain, *Mécanique des Milieux Continus*, Masson, Paris, 1973.
- [5] R. Glowinski, P. Le Tallec, *Augmented Lagrangians and Operator-Splitting Methods in Continuum Mechanics*, SIAM, Philadelphia, PA, 1989.
- [6] E. Guyon, J.P. Hulin, L. Petit, *Hydrodynamique Physique*, EDP Sciences/CNRS Editions, Paris, 2001.
- [7] R. Glowinski, *Finite Element Methods for Incompressible Viscous Flow*, in: P.G. Ciarlet, J.L. Lions (Eds.), *Handbook of Numerical Analysis*, vol. IX, North-Holland, Amsterdam, 2003, pp. 3–1176.
- [8] G. Duvaut, J.L. Lions, *Transfert de chaleur dans un fluide de Bingham dont la viscosité dépend de la température*, *J. Funct. Anal.* 11 (1) (1972) 93–110.
- [9] T.F. Chan, G.H. Golub, P. Mulet, *A nonlinear primal-dual method for total variation-based image restoration*, *SIAM J. Sci. Comput.* 20 (6) (1999) 1964–1977.
- [10] R. Glowinski, *Numerical Methods for Nonlinear Variational Problems*, Springer, New-York, NY, 1984.
- [11] R. Glowinski, J.L. Lions R. Trémolières, *Numerical Analysis of Variational Inequalities*, North-Holland, Amsterdam, 1981.
- [12] J.W. He, R. Glowinski, *Steady Bingham fluid flow in cylindrical pipes: a time dependent approach to the iterative solution*, *Num. Lin. Algebra Appl.* 7 (2000) 381–428.
- [13] M.O. Bristeau, R. Glowinski, *Finite element analysis of the unsteady flow of a visco-plastic fluid in a cylindrical pipe*, in: J.T. Oden, O.C. Zienkiewicz, R.H. Gallagher, C. Taylor (Eds.), *Finite Element Methods in Flow Problems*, University of Alabama Press, Huntsville, AL, 1974, pp. 471–488.
- [14] P.G. Ciarlet, *The Finite Element Method for Elliptic Problems*, North-Holland, Amsterdam, 1978.
- [15] P.G. Ciarlet, *Basic error estimates for elliptic problems*, in: P.G. Ciarlet, J.L. Lions (Eds.), *Handbook of Numerical Analysis*, vol. II, North-Holland, Amsterdam, 1991, pp. 17–351.
- [16] P. Saramito, N. Roquet, *An adaptive finite element method for viscoplastic fluid flows in pipes*, *Comput. Meth. Appl. Mech. Eng.* 190 (40) (2001) 5391–5412.
- [17] J. Cea, R. Glowinski, *Méthodes numériques pour l'écoulement laminaire d'un fluide rigide visco-plastique incompressible*, *Int. J. Comput. Math., Section B* 3 (1972) 225–255.

- [18] G. Vinay, A. Wachs, J.F. Agassant, Numerical simulation of non-isothermal waxy crude oil flows, *J. Non-Newt. Fluid Mech.* 128 (2/3) (2005) 144–162.
- [19] D. Vola, L. Boscardin, J.C. Latché, Laminar unsteady flows of Bingham fluids: a numerical strategy and some benchmark results, *J. Comp. Phys.* 187 (2003) 441–456.
- [20] W.G. Litvinov, R.H.W. Hoppe, Coupled problems on stationary non-isothermal flow of electro-rheological fluids, *Comm. Pure Appl. Anal.* 4 (2005) 776–803.
- [21] J.L. Lions, G. Stampacchia, Variational inequalities, *Commun. Pure Appl. Math.* 20 (1967) 493–519.
- [22] R. Glowinski, Y.A. Kuznetsov, T.W. Pan, On a penalty/Newton/conjugate gradient method for the solution of obstacle problems, *C.R. Acad. Sci. Paris, Série I*, 336 (5), (2003) 435–440.
- [23] B. Dacorogna, R. Glowinski, Y. Kuznetsov, T.W. Pan, On a conjugate gradient/Newton/penalty method for the solution of obstacle problems. Application to the solution of an Eikonal system with Dirichlet boundary conditions, in: M. Krizek, P. Neittaanmaki, R. Glowinski, S. Korotov (Eds.), *Conjugate Gradient Algorithms and Finite Element Methods*, Springer-Verlag, Berlin, 2004, pp. 263–283.
- [24] R. Glowinski, L.J. Shiau, Y.M. Kuo, G. Nasser, On the numerical simulation of friction constrained motions, *Nonlinearity* 19 (2006) 195–216.
- [25] M. Fortin, R. Glowinski, *Lagrangiens Augmentés: application à la résolution numérique des problèmes aux limites*, Dunod, Paris, 1982.
- [26] M. Fortin, R. Glowinski, *Augmented Lagrangians: Application to the Numerical Solution of Boundary Value Problems*, North-Holland, Amsterdam, 1983.
- [27] F.J. Sanchez, Application of a first-order operator splitting method to Bingham fluid flow simulation, *Comput. Math. Appl.* 36 (3) (1998) 71–86.
- [28] E.J. Dean, R. Glowinski, Operator-splitting methods for the simulation of Bingham visco-plastic flow, *Chin. Ann. Math.*, B 23 (2002) 187–204.
- [29] T.C. Papanastasiou, Flow of materials with yields, *J. Rheol.* 31 (1987) 385–404.
- [30] D. Begis, R. Glowinski, Application to the numerical solution of the two-dimensional flow of incompressible visco-plastic fluids, in: M. Fortin, R. Glowinski (Eds.), *Augmented Lagrangian Methods: Application to the Numerical Solution of Boundary Value Problems*, North-Holland, Amsterdam, 1983, pp. 233–255.